

# **Radio Frequency Quadrupole and Alternating Phase Focusing Methods Used in Proton Linear Accelerator Technology in the USSR**

Nikita Wells

**Rand**

The research described in this report was sponsored by the Defense Advanced Research Projects Agency under ARPA Order No. 3520-17, Contract MDA903-82-C-0067, Director's Office.

**Library of Congress Cataloging in Publication Data**

Wells, Nikita, 1937-

Radio frequency quadrupole and alternating phase focusing methods used in proton linear accelerator technology in the USSR.

"Prepared for the Defense Advanced Research Projects Agency."

"R-3141-ARPA."

1. Proton accelerators. 2. Ion bombardment—Research—Soviet Union. 3. Linear accelerators. 4. Particle beams—Technique. I. United States. Defense Advanced Research Projects Agency. II. Title.

QC787.P7W45 1985 539.7'33 84-11699

ISBN 0-8330-0579-0

The Rand Publication Series: The Report is the principal publication documenting and transmitting Rand's major research findings and final research results. The Rand Note reports other outputs of sponsored research for general distribution. Publications of The Rand Corporation do not necessarily reflect the opinions or policies of the sponsors of Rand research.

# **Radio Frequency Quadrupole and Alternating Phase Focusing Methods Used in Proton Linear Accelerator Technology in the USSR**

Nikita Wells

January 1985

Prepared for the  
Defense Advanced Research  
Projects Agency



APPROVED FOR PUBLIC RELEASE: DISTRIBUTION UNLIMITED



## PREFACE

This report was prepared in the course of a continuing study, sponsored by the Defense Advanced Research Projects Agency, of Soviet research and development of high-current, high-energy, charged particle beams and their scientific and technological applications. The report examines Soviet research on (1) the radio frequency quadrupole and (2) the alternating phase focusing methods of accelerating and focusing proton (and heavy ion) beams in linear accelerators, as reported in Soviet open-source technical publications.

The report is the third in a series by the present author on the subject of generating and accelerating intense ion and neutral particle beams. The first report was *The Development of High-Intensity Negative Ion Sources and Beams in the USSR*, R-2816-ARPA, November 1981; and the second, *Production of Neutral Beams from Negative Ion Beam Systems in the USSR*, R-2909/1-ARPA, December 1982. All three reports should be of interest to analysts involved in pulsed-power and energy-related research.



## SUMMARY

Soviet development of ion induction linear accelerators has been remarkable in its steady pursuit of such goals as high current levels, reliability, efficiency, reduced size, and simplicity of operation. In the course of this development, the Soviets have made several significant contributions to ion linac technology, such as the invention of the high-brightness, surface-plasma ion source, the radio-frequency quadrupole (RFQ) system, and the gyrocon power source. While Soviet publications acknowledged only synchrotron accelerators and high-energy physics experiments as the ultimate applications of these inventions, the latter, as well as the goals characterizing Soviet ion linac development, appear singularly applicable to the task of propagating particle beams in space.

The RFQ system has been especially effective in providing the practical means of approaching the space propagation criteria of high current level, low injection energy, adequate reliability, efficiency, and moderate size. It has been the object of an intensive Soviet development effort since its invention, and led to the capability to pass 100 mA currents at RFQ output of 2 to 3 MeV for input energies as low as 100 keV. Another method of simultaneous acceleration and focusing of ions under Soviet development has been the alternating phase focusing (APF) system, which has recently achieved a successful feasibility proof.

The present report analyzes the Soviet development of the RFQ and APF systems as reflected in the Soviet open-source technical literature published over the past 15 years. While these systems are essentially capable of accelerating and focusing positively and negatively charged particles, Soviet publications omit the consideration of negative ions in the context of RFQ and APF development, even though negative ions are particularly important to the formation of intense high-energy neutral particle beams. Consequently, this report is likewise limited to the consideration of protons and heavy ions as the particle species subject to acceleration and focusing by the RFQ and APF systems.

Soviet development of the RFQ and APF systems has been carried out by several major Soviet research institutes of the Academy of Sciences, USSR, and the universities: Institute of Theoretical and Experimental Physics (ITEF), Institute of High-Energy Physics (IFVE), the Nuclear Research Institute (IYAI), Radiotechnical Institute (RAIAN), Khar'kov Physico-technical Institute (KhFTI), and Moscow Engineering Physics Institute (MIFI). The work of these organizations has

been characterized by fairly clear division of labor and dedication to separate major development projects. The first three institutes pursued the development of the RFQ system, while RAIAN was the main developer of the APF; the latter effort was recently joined by KhFTI and MIFI. The division of labor is further manifested by the different functions of each institute: Among the major accelerator systems, IFVE has been developing the 30 MeV URAL injector, and a 50 MeV injector is planned at ITEF; theoretical analyses have been provided by IYAI for RFQ systems and by KhFTI for APF systems.

At IFVE, the RFQ is used in the initial section of the URAL-30 injector. A proton current of 130 mA has been successfully passed through the RFQ structure, while 80 mA passed through the entire injector at 30 MeV. The major issue at IFVE is the matching of the beam to the accelerator in order to minimize beam emittance and its dependence on the phase of injected particles. ITEF, developing the preinjector stage for its 50 MeV system, has focused on the problem of electrode shape, and has found the semicircular cylinder with a sinusoidal transition section to be the optimal shape. The focusing effectiveness, linearity of the electric field, and transit time of the particles due to the optimal electrode shape have been found close to the theoretical electrode values. The ITEF electrode solution has also proved to be successful in engineering terms: The electrode machining operation is claimed to be relatively simple and has been performed both manually and by a computer-controlled milling machine.

RAIAN's development of the APF system was initially limited to low beam currents of about 40 mA. However, KhFTI has reported on the possibility of obtaining limiting beam currents as high as 350 mA, and RAIAN suggested that a hollow beam version of the APF could reach a current of 500 mA. An alternative method of increasing the beam current limit, suggested by RAIAN, is based on accelerating separate beamlets through multiple apertures in the drift tubes. In this manner, beam currents from 300 to 400 mA are expected to be possible for beam injection energies as low as 200 keV. The multiple beamlet system is deemed by the Soviets to be particularly suitable for the acceleration of heavy ions. This system is also claimed to be the best means of realizing accelerating voltage gradients of 13 MV/m in proton linac injectors.

An injector based on the APF system has recently been put into operation at MIFI. This is a 1.2 MeV proton linear accelerator with an injection energy of 100 keV, and an injected beam current of up to 120 mA and 150  $\mu$ s pulse-length. The MIFI injector thus appears to demonstrate the practical feasibility of the APF system.

Tables S.1 and S.2 show the chronology of development of the Soviet RFQ and APF acceleration and focusing system for high current proton and ion beams.

Table S.1  
CHRONOLOGY OF SOVIET RFQ DEVELOPMENT

Year	Insti- tute	R and D Objective	System	Beam Parameters					
				Energy					
				RFQ Input	RFQ Output	Injector Output	Beam Current	Pulse Length	Beam Emittance
1970	ITEF	Initial RFQ theory							
1972	IFVE	1st RFQ test with I-100 preinjector (horn drift tube)		510 keV	3.26 MeV		100 mA	40 $\mu$ s	1 cm-mrad
1974	IFVE	2d RFQ test with URAL preinjector (spatially uniform structure)		100 keV	620 keV		200 mA	10 $\mu$ s	.46 cm-mrad at 100 mA
1975	IFVE	1st linac stage of linear accelerator	URAL-15	100 keV	2 MeV	15 MeV	50 mA	10 $\mu$ s	.3 cm-mrad at 40 mA
1976	ITEF	Deuteron linac with RFQ for neutron generator-proposal			3 MeV <sup>a</sup>	100 MeV <sup>a</sup>	250 mA <sup>a</sup>		
1977	IFVE	2d linac stage of linear accelerator	URAL-30	100 keV	2 meV	30 meV	100 mA <sup>a</sup>	10 $\mu$ s <sup>a</sup>	

Table S.1—continued

Year	Insti- tute	R and D Objective	System	Beam Parameters					
				Energy			Injector Output	Beam Current	Beam Emittance
				RFQ Input	RFQ Output	2 MeV			
1977	IFVE	RFQ test	URAL-30	100 keV	2 MeV		130 mA	5 $\mu$ s	.3 cm-mrad
1980	ITEF	RFQ electrode shape design							
1980	IYAI	RFQ simulation with LINUS code							
1980	IFVE	Operation of linear accelerator	URAL-30	100 keV	2 MeV	30 MeV	80 mA	5 $\mu$ s	.5-1 cm-mrad
1981	IFVE	RFQ beam matching for URAL-30	URAL-30						
1982	ITEF	RFQ injector		92 keV	3 MeV	50 meV <sup>a</sup>	100 mA	25 $\mu$ s	

<sup>a</sup>Proposed.

Table S.2  
CHRONOLOGY OF SOVIET APF DEVELOPMENT

Year	Insti- tute	R and D Objective	Beam Parameters			
			Injector Energy		Beam Current	Beam Emittance
			Input	Output		
1969	RAIAN	Early APF theory	(15-50 mA max)			
1972	RAIAN	1st APF test using AAPF method	50 keV	550 keV	1 mA	.36 $\pi$ cm-mrad
1975	RAIAN	AAPF theory: particle dynamics as a function of aperture size	(100 keV)	(1.8 MeV)		
1976	RAIAN	2d APF test using AAPF method	100 keV	1.8 MeV	1 mA	
1977- 1979	RAIAN	Multiple aperture beams, AAPF theory (also heavy ions)	(200 keV)	(1 MeV, 20 MeV)	(300-400 mA max)	2.4 $\pi$ cm-mrad

Table S.2—continued

Year	Insti- tute	R and D Objective	Beam Parameters			
			Injector Energy		Beam Current	Beam Emittance
Input	Output					
1978	RAIAN	Hollow beam APF theory			(500 mA max)	
1977- 1982	KhFTI	APF optimization theory comparison of AAPF and MAPF methods	(150 keV)	(3 MeV)	(350 mA max for MAPF)	
1981	MIFI	Proton injector operation using AAPF method	100 keV	1.2 MeV	Up to 120 mA, 150 $\mu$ s at input	.16 $\pm$ .02 cm-mrad

NOTE: Figures in parentheses are theoretical values only.



## ACKNOWLEDGMENTS

The author would like to thank Richard H. Stokes, Thomas P. Wangler, and Kenneth R. Crandall of the Los Alamos National Laboratory for their reviews of this report and for their many helpful suggestions. He is also grateful to his colleagues at The Rand Corporation: Robert W. Salter for reviewing the report, and Simon Kassel for direction, support of, and interest in the project.

The author thanks Plenum Publishing Corporation for permission to reproduce graphics taken from two Soviet scientific journals: from *Soviet Apparatus and Experimental Techniques* (*Pribory: tekhnika eksperimenta*), graphics appearing herein as Figs 1, 2, 28, 39, 40, and 41. And from the *Soviet Atomic Energy Journal* (*Atomnaya energiya*), graphics appearing herein as Figs. 10-18, 43-45.

The American Institute of Physics kindly granted permission to reproduce graphics taken from three Soviet scientific journals: from *Soviet Physics—Technical Physics* (*Zhurnal technicheskoy fiziki*), graphics appearing herein as Figs. 19-27, 31-37, 42, 48-52; from *Soviet Technical Physics Letters* (*Pis'ma v zhurnal technicheskoy fiziki*), graphics appearing herein as Figs. 29, 30; and from *Advances of Physical Sciences* (*Uspekhi fizicheskikh nauk*), graphics appearing herein as Figs. 3, 4.



## CONTENTS

PREFACE .....	iii
SUMMARY .....	v
ACKNOWLEDGMENTS .....	xiii
FIGURES .....	xvii
TABLES .....	xxi
Section	
I. INTRODUCTION .....	1
II. RADIO-FREQUENCY QUADRUPOLE FOCUSING .....	3
II.1. RFQ Development at ITEF .....	3
II.2. RFQ Injector Operation at ITEF .....	6
II.3. RFQ Development at IFVE .....	12
II.4. RFQ Injector Operation at IFVE .....	24
II.5. Theoretical Calculations on RFQ Focusing and Acceleration at IYAI .....	32
II.6. Double-Component Ion Beams .....	39
III. ALTERNATING PHASE FOCUSING .....	44
III.1. Background and Early Research on APF .....	44
III.2. APF Research at RAIAN .....	45
III.3. APF Research at KhFTI .....	50
III.4. APF Research at MIFI .....	55
IV. CONCLUSIONS .....	62
REFERENCES .....	65

## FIGURES

1. Four-Element Electrodes with the Quadrupole Symmetry . . . . .	3
2. Electrode Cross-section in the Two Orthogonal Planes . . . . .	4
3. Volume Resonator Cross-section for Accelerating Structures having Spatially Homogeneous Quadrupole (RFQ) Focusing . . . . .	5
4. Accelerator Section with RFQ Focusing . . . . .	6
5. Initial Accelerator Section of the New Proton Injector Being Assembled at ITEF, Showing the RFQ Structure . . . . .	8
6. Details of the Final Section of the RFQ Structure Showing the Electrodes . . . . .	9
7. Cylindrical Variable-Diameter Electrodes with Conical Transitions . . . . .	10
8. Semicircular Electrodes with Sinusoidal Transitions . . . . .	11
9. Increase in Phase Space in the I-2 Linear Accelerator . . . . .	13
10. Block Diagram of the Experimental Apparatus . . . . .	13
11. Accelerated Beam Current as a Function of Injection Current .	14
12. Capture Coefficient as a Function of RF Power . . . . .	15
13. Acceptance of the Accelerator . . . . .	16
14. Schematic of the IAS Beam Analyzing Apparatus . . . . .	17
15. Accelerated Beam Current as a Function of Injected Beam Current . . . . .	18
16. Accelerated Beam Current as a Function of the RF Voltage Level ( $I_{inj} = 300$ mA) . . . . .	18
17. Spectra of the Accelerated Beam . . . . .	19
18. Beam Emittance Measurements at the Output of the RFQ .	20
19. RFQ Electrode Shape and Cross-Section of Resonators with the Matching Section Connected to the Input of the RFQ Accelerating Electrodes . . . . .	21
20. RFQ Acceptance Curves as a Function of Input Phase (in radians) without a Matching Section and with a Matching Section . . . . .	22
21. Emittance Diagram for a Beam at the Output of the RFQ for an Input Emittance of $E_{in} = 0.35$ without a Matching Section and with a Matching Section . . . . .	23
22. Block Diagram of the URAL-30 Accelerator . . . . .	25
23. Block Diagram of the URAL-30 Accelerator, Electrode Shape, and Cross-Section of the Resonators . . . . .	27
24. Beam Emittance at the Output of the URAL-15 Accelerator .	28
25. Accelerated Beam Particle Spectra at Different Acceleration Conditions . . . . .	29

26. The MAS Accelerator System with the H-Resonator . . . . .	30
27. Distribution of Amplitudes of the Applied Accelerating Electric Field as a Function of Gap Number Along the Accelerating System Axis . . . . .	30
28. Mounting Stand for Electrode Alignment . . . . .	31
29. Normalized Beam Emittance as a Function of Beam Current .	33
30. Beam Emittance Diagram at the Output of the Accelerator with a Beam Current of 200 mA . . . . .	34
31. Beam Radius Behavior Along the Axis of the Accelerator at Different Beam Currents . . . . .	35
32. Partial Beam Emittance at the Accelerator Output as a Function of Injected Beam Current . . . . .	35
33. Beam Current as a Function of Normalized Beam Emittance at the Accelerator Input, and Output at an Injection current of 200 mA . . . . .	36
34. Phase Diagram of a Bunched Beam in the x, x' Plane . . . .	38
35. Phase Space Diagrams Showing Beam Matching . . . . .	40
36. Dependence of the Particle Capture Coefficient as a Function of Injected Beam Current . . . . .	41
37. Capture coefficient $k_{H^-}$ and $k_{H^+}$ as Functions of $H^-$ Ion Beam at Different Intensities of the Proton Beam . . . . .	42
38. Dependence of the Effective Emittance $E_{H^-}$ at the Buncher Exit as a Function of the Injected $H^-$ Beam Current . . . . .	43
39. Multiple Beam Accelerating Structure . . . . .	48
40. Schematic of the Multiple Beam Combination Apparatus .	49
41. Diagram of the Beams in the Geometric and Orthogonal Phase Planes Before and After Combination . . . . .	49
42. Change in the Synchronous Phase $\Delta\varphi$ as a Function of $\beta/\beta_s$ .	51
43. Lateral Acceptance of the MLUD-3 Accelerator for an Energy Spread at the Input Within the Limits of $\pm 1$ Percent . . . .	52
44. Accelerated Ion Beam Current as a Function of Injection Current . . . . .	52
45. Dependence of the Accelerated ion Beam Current as a Function of the Maximum Initial Trajectory Angle of the Particles . . . . .	53
46. Areas of Phase Capture for the AAPF and the MAPF Cases .	54
47. Accelerated Beam Currents for the AAPF and the MAPF Cases . . . . .	54
48. Overall Schematic of the Accelerator System . . . . .	56
49. Schematic Diagram of the 1.2 MeV Accelerator Using AAPF Put into Operation at MIFI . . . . .	57



50. Distribution of the Electric Field Strengths Along the Length of the Resonator . . . . .	58
51. $\Delta\beta/\beta s$ as a Function of $\Delta\varphi$ . . . . .	59
52. Accelerator Acceptances for Various Injection Phases of the Particles . . . . .	60



## TABLES

S.1. Chronology of Soviet RFQ Development . . . . .	viii
S.2. Chronology of Soviet APF Development . . . . .	x
1. Basic Parameters of the Horn Drift Tube RFQ at IFVE . . . . .	14
2. Basic Parameters of the RFQ used in the Preinjector	
Section at IFVE . . . . .	21
3. Basic Parameters of the URAL-30 Injector System . . . . .	26
4. Basic Parameters of the 1.2MeV Accelerator Using	
AAPF Put into Operation at MIFI . . . . .	56
5. Particle Phase Values for Each Acceleration Gap in	
the Accelerator . . . . .	59



## I. INTRODUCTION

This report covers Soviet development of those aspects of ion linear accelerators that are relevant to the problem of particle-beam propagation in space. Generation of high-current beams of neutral particles capable of long-distance propagation in space requires an efficient and relatively compact linear accelerating system (linac) in which ions are subject to the accelerating forces. The ion linac technology has been developed in the past primarily to study high-energy physics phenomena, involving very large and complex accelerating structures. Their size and complexity are not of primary consideration in this application. They are, however, a major hindrance to the development of spaceborne sources of neutral beams. Another basic difference between the high-energy physics and space propagation applications of particle accelerators resides in the level of beam current. High-energy physics experiments have been performed with the beam currents in the range from  $\mu$ A to low mA. On the other hand, space propagation may require currents from 100 mA upwards. While space application of particle beams has never been explicitly acknowledged in Soviet open sources, high beam intensity, low beam emittance, simplicity, small size, economy, and manageability have all been goals of Soviet development efforts carried on since at least the late sixties in the area of ion linear accelerators. In the course of this effort, the Soviets invented the radio-frequency quadrupole (RFQ) system and independently developed the alternating phase focusing (APF) system, either of which provides the means to accelerate and focus intense ion beams. The RFQ or the APF system is used in the front end of the accelerator in conjunction with further acceleration stages using cylindrical resonators or drift tubes with permanent magnet quadrupole lenses. The specific advantages of these two systems include low injection energy, small resonator size, and absence of magnetic focusing, as well as overall compactness and simplicity of construction.

The RFQ system has now provided proton and deuteron beams with currents as high as 200 to 300 mA, obtained with injection energies as low as 70 to 100 keV. Both the RFQ and APF systems have demonstrated the ability to accelerate very heavy particles, such as uranium ions, where almost 100 percent capture can be achieved because of the high acceptance efficiency for low-velocity ions. Acceleration of intense  $H^-$  ion beams is also possible with these systems. Negative ion beam systems are important in the generation of intense neutral

particle beams, because of the high conversion efficiency of negative ions into neutrals at higher energies. The low conversion coefficient of positive ions above 120 keV practically precludes their use for this purpose.

The RFQ system became the subject of U.S. development in 1978 at the Los Alamos National Laboratory, where it has become an important component of linear accelerators for many applications. It has recently also gained acceptance in a number of laboratories in the West.

In the APF system, the basic structure of the important elements is considerably simpler than that of the RFQ system. However, the choice of the interacting parameters, which determine the longitudinal and transverse particle motion, is more complex. While the APF system has been under continuous development in the Soviet Union since 1969, it has received much less attention in the West.

Soviet research on high-intensity proton linear accelerators has been performed at the Radiotechnical Institute of the Academy of Sciences (RAIAN) in Moscow, the Institute of High-Energy Physics (IFVE) in Protvino, and the Institute of Theoretical and Experimental Physics (ITEF) in Moscow. Additional theoretical and experimental studies have been carried out at the Institute of Nuclear Research (IYAI) of the Academy of Sciences in Moscow, the Moscow Engineering Physics Institute (MIFI), and the Khar'kov Physico-technical Institute (KhFTI). The work on RFQ systems has been done at ITEF, IFVE, and IYAI in association with the development of injectors for proton synchrotrons. The research on APF has been concentrated at RAIAN, where this mode of focusing has been studied since 1969 to the present. Only relatively recently (since 1977), additional research on APF has been carried out at KhFTI, where a comparison was made of the two alternative systems, and at MIFI, where a new proton linear accelerator with APF was put into operation in 1981.

The present report provides a detailed analysis of the effort of these institutes in developing the RFQ and APF systems and producing high-intensity ion beams. The input materials used in this report are limited to open-source literature, primarily in the form of research reports of the Soviet performer institutes, published between 1968 and 1983. The structure of the report is as follows: Section II covers the RFQ system, analyzing prototype development and accelerator structure at ITEF and IFVE, providing an account of RFQ theory at IYAI, and concluding with the principle of simultaneous acceleration and focusing of positive and negative ion beams (double-component principle). Section III deals with the APF system development at RAIAN, KhFTI, and MIFI, and Section IV provides conclusions.

## II. RADIO-FREQUENCY QUADRUPOLE FOCUSING

### II.1. RFQ DEVELOPMENT AT ITEF

The principle of "spatially uniform quadrupole focusing" as developed by Soviet researchers is more commonly referred to as "radio-frequency quadrupole focusing" (RFQ) in the United States. RFQ focusing was invented at ITEF and first investigated in the late 1960s [1,2] by I. M. Kapchinskiy and V. A. Teplyakov. Here they first proposed the combined function of beam focusing and acceleration in a linear ion accelerator. The focusing and acceleration function is accomplished by a high-frequency (RF) electric field generated by four-element (quadrupole) long electrodes. The focusing effect is obtained by the application of a time-changing potential on the quadrupole electrodes; the system is homogeneous along the axis of the accelerator, as shown in Fig. 1 [1].

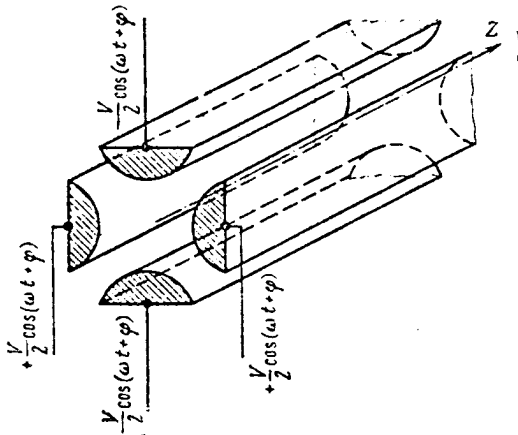


Fig. 1—Four-element electrodes with the quadrupole symmetry [1]

The high-frequency potential  $(\pm V/2) \cos(\omega t + \varphi)$  imposes alternating polarity gradients on particles moving along the axis, resulting in a sharp focusing effect [1].

The researchers at ITEF then showed that in addition to the focusing forces, one can obtain longitudinal accelerating forces with the high-frequency focusing fields if the distance between opposite electrodes of similar polarity is periodically changed along the axis. The spatial period of the electrode structure must be equal to the distance covered by a design particle during this high-frequency interval. The vertical and horizontal planes must be shifted relative to each other by one-half a spatial period. The potential of the electric field on the axis then is found to be modulated by a period of  $\beta\lambda$ , which produces the resonant accelerating effect [1]. The cross-section of the electrodes along the beam axis in the horizontal and vertical planes is shown schematically in Fig. 2. Here the beam axis lies along the  $z$  axis, and  $k$  is the wave number,  $k = 2\pi/\beta\lambda$ .

With a given channel aperture, the acceleration effectiveness increases with a large increase in the degree of modulation but the focusing effectiveness decreases. Thus, there exists an optimum modulation distance between electrodes. As it was determined through calculations at ITEF [1], the average increase in proton energy per unit length in the proposed system was found to be about 1 MeV/m, and

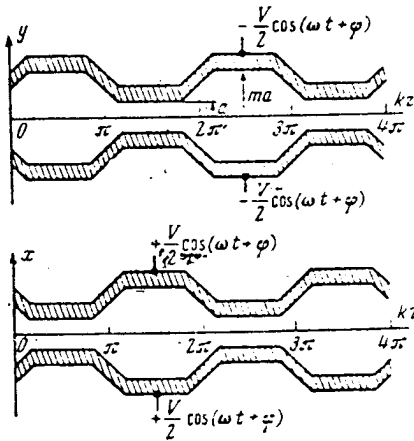


Fig. 2—Electrode cross-section in the two orthogonal planes [1]

the conductance (the normalized acceptance) was determined to be about 1.5 cm-mrad up to an energy of 20 to 30 MeV with a maximum value of RF field up to 250 kV/cm. The values of these fields are now being used in present-day accelerators. The acceleration system can be effectively used at low injection energies of 100 to 200 keV because of the spatial continuity of the focusing and accelerating structure and because the average increase of energy per unit length at low energies is increased considerably.

The behavior of the beam in a spatially homogeneous (RFQ) strong focusing channel possesses special characteristics. The matched beam has a constant size along the axis of the channel. In each of the planes the maximum cross-section dimension appears at the moment in time when the channel in the corresponding plane is focusing, and the minimum dimension appears when the channel is defocusing. The conditions of beam matching at the input to the channel changes periodically with the frequency of the electric field. Thus, it is necessary to dynamically match the beam to the channel. This matching can be made by using RF quadrupole lenses [1] or the matching section as described in Sec. II.3.

The four-element line can be energized in the resonator with a longitudinal magnetic field. Various types of resonators with a quadrupole-type wave are shown in Fig. 3. The double H-resonator is shown in Fig. 3a. Two types of four-chamber resonators, namely the

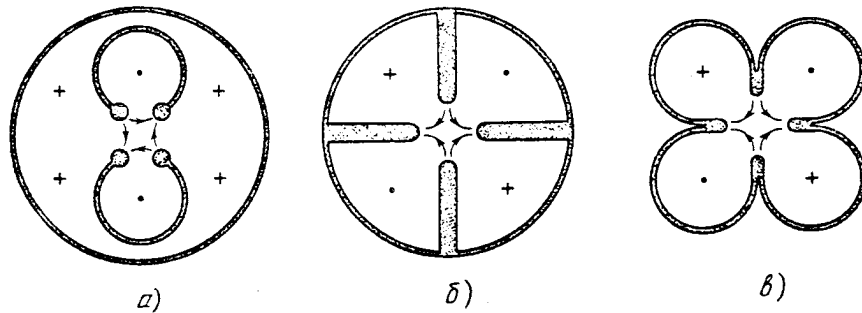


Fig. 3—Volume resonator cross-section for accelerating structures having spatially homogeneous quadrupole (RFQ) focusing [3]  
 a—double H-resonator  
 b and c—two types of four-chamber resonators

sectorial and the cloverleaf, are shown in Fig. 3b and Fig. 3c, respectively [3,4]. The figure also shows the direction of the electric field near the axis and the magnetic field in the resonating volumes. A photograph of a single section of an accelerator with RFQ focusing is shown in Fig. 4.

## II.2. RFQ INJECTOR OPERATION AT ITEF

The RFQ accelerator structure at ITEF is presently being incorporated into the new proton synchrotron injector intended to replace the now obsolete 25 MeV I-2 linear accelerator.

The new proton injector, now under development, is expected to reach an output energy of 40 to 50 MeV as compared with the 24.6 MeV of the I-2, and to have improved beam parameters [5]. The accelerator consists of an initial RFQ section followed by an Alvarez-type resonator operating with a double frequency of 297 MHz and using permanent magnet quadrupole lenses, which will provide focusing of the beam. The transition energy between the RFQ and the Alvarez structure was chosen as 3 MeV for optimum beam transmission. The

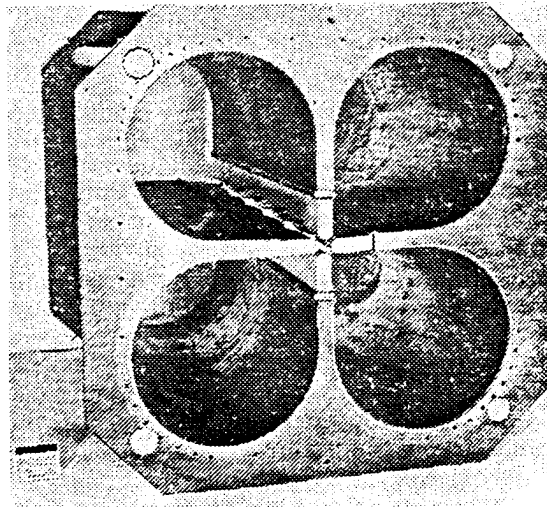


Fig. 4—Accelerator section with RFQ focusing [3]

RFQ structure was aligned and tuned in 1981. The initial section of the accelerator showing the RFQ resonator and vacuum chamber is shown in Fig. 5 [5].

The resonator is composed of eight separate sections, each from 574 to 602 mm long. Each of the four chambers includes tuning plates, an electrode translation mechanism, and current measuring loops. The matching of the beam along longitudinal and transverse coordinates from the RFQ to the linac is accomplished by an adiabatic change of parameters along the initial part of the first section. Details of the RFQ structure showing the accelerating and focusing electrodes are shown in Fig. 6 [5].

The Soviet researchers recognized that the cloverleaf-type RF-chamber resonators are the most convenient configuration for providing the required quadrupole fields, since the RF field is concentrated inside a single closed cavity and thus optimizes on the cooling of the resonator. The four-chamber resonator with longitudinal magnetic field has been analyzed in detail at ITEF [6]. IFVE, however, is using the double H-resonators.

ITEF started operating the 3 MeV RFQ accelerator in October 1982, and obtained a proton beam current of 100 mA with a pulse length of 25  $\mu$ s [7]. The measurement of protons having energy of 3 MeV was confirmed by passing the beam through a stainless steel foil. The optimum beam injection energy was determined to be 92 keV and the beam output momentum spread was less than 3 percent [7]. The structure of the RFQ accelerator consists of three sections: the matching section, the buncher, and the main accelerator section. The matching section comprises 22 cells, where transverse matching is accomplished by reducing the distance between the electrodes. To optimize the particle capture in this section, the equilibrium phase is maintained at a value of  $-90^\circ$ . In the buncher section the beam is broken up, bunched, and further accelerated while maintaining constant space-charge density. The output section of the buncher imposes a limit on the maximum beam current pulse. The equilibrium phase in the main accelerator section is  $-35^\circ$  with a maximum accelerating field of 250 kV/cm and a maximum voltage between adjacent vanes of 185 kV [7].

A hollow cold cathode duoplasmatron ion source was used with the injector and was located at a minimal distance of about 30 cm from the linear accelerator input.

Another RFQ application was studied at ITEF in 1976-1977, involving an intense pulsed proton linear accelerator employing double frequency with a final energy of 100 MeV [8]. This accelerator is expected to accelerate deuterons for use as an intense neutron generator in [9]. A 250 mA beam current was envisaged for the RFQ using a

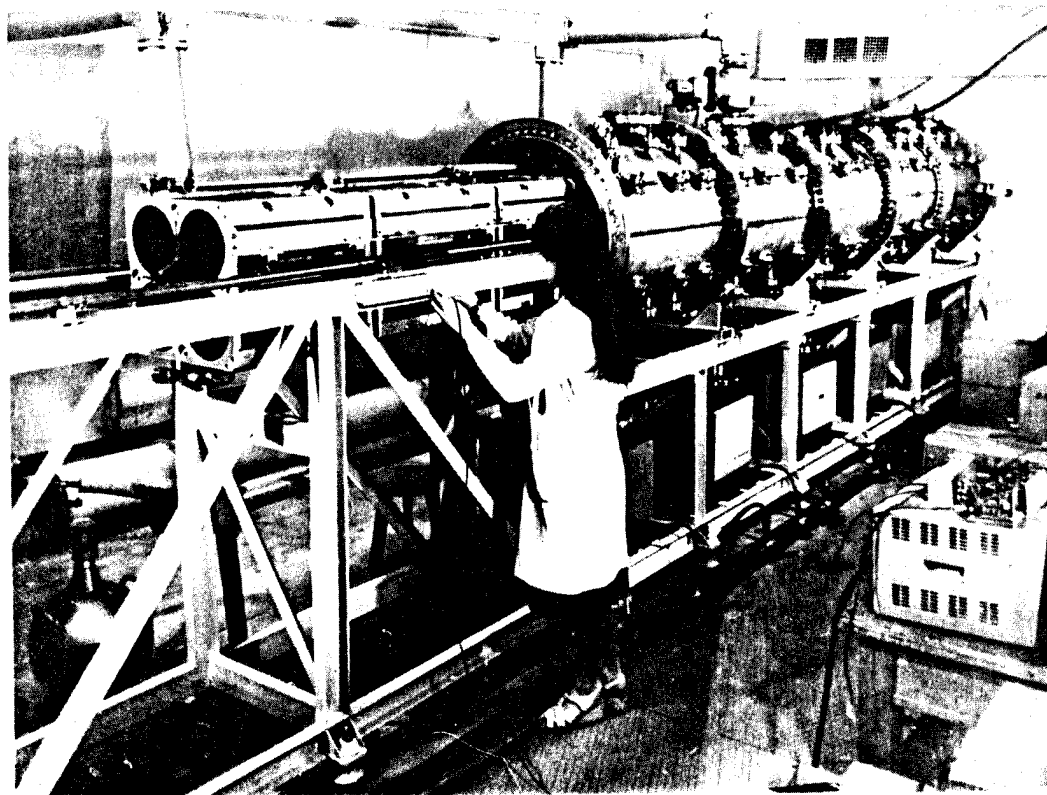


Fig. 5—Initial accelerator section of the new proton injector  
being assembled at ITEF, showing the RFQ structure [5]

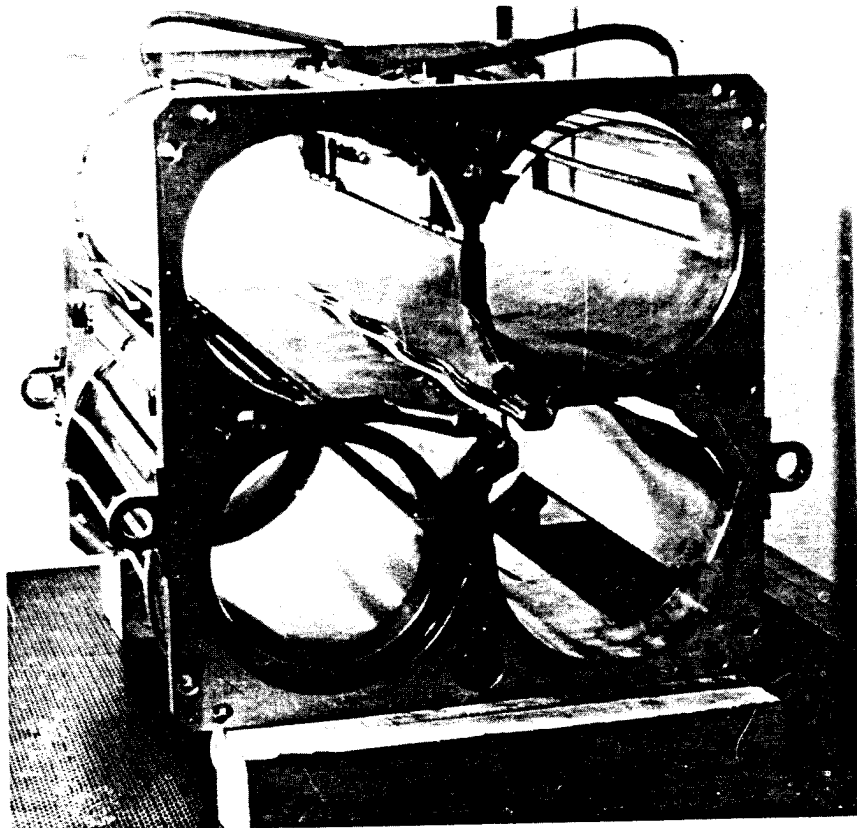


Fig. 6—Details of the final section of the RFQ structure showing the electrodes [5]

2 m accelerating wavelength. The RFQ section would accelerate the beam to an energy of 2.5 to 3 MeV, beyond which the beam would further be accelerated using cylindrical resonators with drift tubes with a 1 m wavelength accelerating field. After the 3 MeV point, particles in the beam experience less coulomb repulsion; there is no loss in beam intensity.

The wavelength change from 2 m to 1 m at the end of the RFQ section decreases not only the resonator length but also its diameter. The voltage between adjacent electrodes in the RFQ is set at 188 kV with a maximum electric field of 235 kV/cm at the electrode surfaces [8]. The final section would have 56 drift tubes with permanent magnet quadrupoles that produce a focusing magnetic field gradient changing from 5.8

to 2.3 kG/cm. The average axial field will be 35 kV/cm with a gap coefficient  $\alpha = 0.3$  and a maximum electric field at the electrode surface of 235 kV/cm, the same as the value in the RFQ.

The total length of the proposed accelerator, including the ion source and its power supplies, will be 15 m, which corresponds to an average acceleration rate of 1.67 MeV/m. In comparison, the average acceleration rate of the I-2 accelerator is only 0.82 MeV/m [8].

The effectiveness of acceleration and focusing in various RFQ focusing electrode structures was analyzed theoretically by ITEF in 1980 [10] and in 1981 [11]. According to ITEF, the fabrication of desirable RFQ electrode surfaces is limited by the constraint imposed upon the electrode spacing by the distance between poles required to maintain the appropriate electrode voltage without sparkover. ITEF considered various electrode shapes in order to improve the accelerator performance. Two types of RFQ electrode pole shapes have been carefully studied: variable-diameter cylindrical electrodes with conical transitions (Fig. 7) and semicircular electrodes with sinusoidal transitions (Fig. 8). The results of the analysis have been compared with formulas based on ideal electrodes.

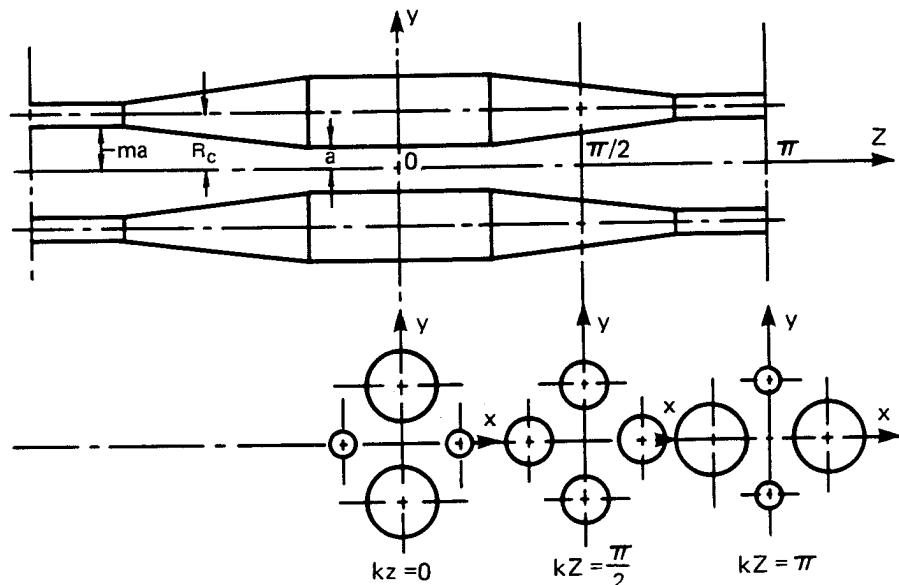


Fig. 7—Cylindrical variable-diameter electrodes with conical transitions [10]

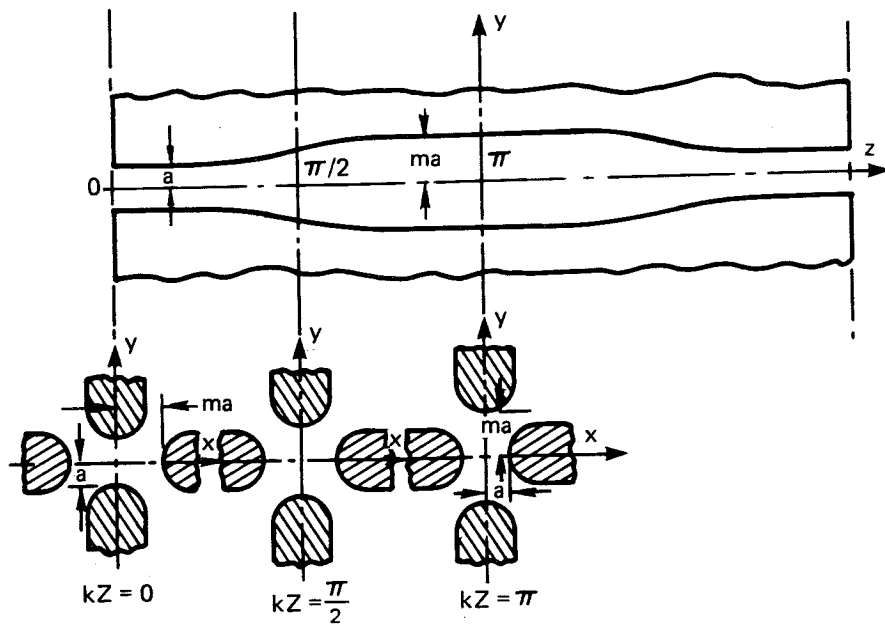


Fig. 8—Semicircular electrodes with sinusoidal transitions [10]

The resulting equations represent approximations to the ideal electrode shape, and the errors introduced by these formulas depend on the degree of such approximation. Semicircular-shaped electrode poles with sinusoidal transitions are found to provide the optimum practical geometry.

The focusing field created by the semicircular electrodes, with a ratio of electrode radius to average distance from the axis to the electrode of about 1.14, was found to possess the best linearity. Therefore, ITEF decided to use half-cylindrical electrodes with constant thickness and sinusoidal modulation of the distance between the electrodes and the axis. ITEF points out that the focusing effectiveness of the transit-time factors turns out to be close to the theoretical values. The equipment and techniques for fabricating these electrodes were reported to be relatively simple [5]. The electrodes were machined both by hand and by a computer-controlled milling machine.

The old 25 MeV, I-2 linear accelerator was initially set into operation in 1966 [12] and has been operating with pulsed beam currents ranging from 160 to 180 mA with maximum of 200 mA [13,14]. The

accelerator, in addition to its function as an injector for the proton synchrotron, has been used to propagate its beam in the atmosphere for a series of various experiments [13,15]. The I-2 accelerator operated either as the injector to the synchrotron with intermittent pauses of 0.8 and 3.2 s or by itself with a repetition rate of 1 Hz and a pulse length of 3 to 50  $\mu$ s. The I-2 accelerator was thus used as an injector or as an intense source of protons [15]. The proton beam was injected into the atmosphere through an aluminum foil 0.3 mm thick. Experiments with beam injection into air started in October 1971 with beam currents greater than 100 mA.

Detailed beam emittance measurements made recently in [16] showed that the beam emittance was actually lower than 1.2 cm-mrad for beam currents of up to 190 mA, with an injected beam current of 460 mA for 95 percent beam sampling. The matching channel of this accelerator had to be totally reconstructed after tests showed that the injected beam current of up to 400 mA did not raise the value of the output beam current above 200 mA. This problem was solved mainly by increasing the beam apertures of the quadrupole lens electrodes to an internal diameter of 9 cm [17,14,18].

The larger the acceptance of the linear accelerator and the larger the phase density of the beam, the higher the coulomb limit of the beam and thus the beam current that can be passed through the linear accelerator. The acceptance of an Alvarez-type linear accelerator is approximately proportional to the cube of the accelerating field wavelength, thus providing an effective means of increasing the pulsed beam intensity by increasing the wavelength. Countering this advantage, however, is the fact that the total cost of the accelerator increases with wavelength.

It was determined at ITEF that at relatively high energies (about 10 MeV), the emittance of the core of the beam does not change and the increase in phase space is due solely to the halo of the beam. The experimental results of Fig. 9 show the absence of change in the phase space of the core containing 80 percent of the particles [19,20]. The left-hand curve shows a 400 mA beam at the input to the accelerator and the right-hand curve shows a 180 mA beam at the output to the accelerator. Here the beam core phase space remains unchanged while the halo phase space increases and, at the end of the acceleration, reaches the acceptance value set for the whole beam.

### II.3. RFQ DEVELOPMENT AT IFVE

The first experimental investigation of the acceleration and focusing of a proton beam using an RFQ structure was carried out at IFVE in

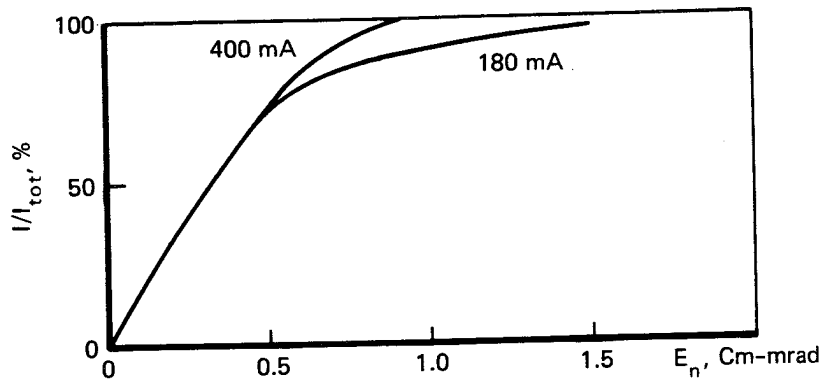


Fig. 9—Increase in phase space in the I-2 linear accelerator [19]

1972 [21]. This RFQ structure utilized horns mounted at the faces of drift tubes as described later in this section. The preinjector of the I-100 linear accelerator was used to inject a 100 mA proton beam at 500 to 600 keV into the section under test. A 25 mA, 3.26 MeV proton beam was obtained at the output of the RFQ section and was limited only by the 100 mA beam—the maximum that could be obtained from the injector. A block diagram of the apparatus used to accelerate protons is shown in Fig. 10 [21]. The accelerator section, with the RFQ electrodes and resonator, was housed in a vacuum chamber that also served as a shield made up of three separate sections measuring 70 cm long. The acceleration electrodes used here were of the double-gap type [22] and the resonator was the H type [23].

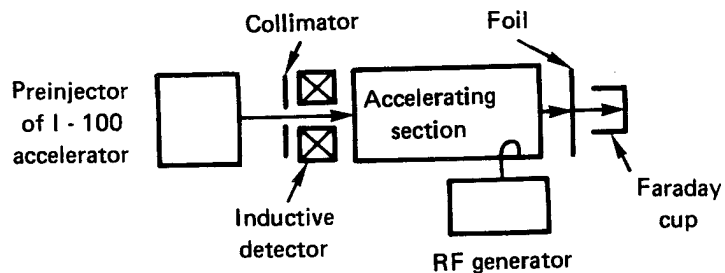


Fig. 10—Block diagram of the experimental apparatus [21]

The basic parameters of the RFQ section are given in Table 1 [21]. The beam current at the input to the accelerator was measured by an inductive detector and at the output by a faraday cup, which had a removable foil in front of it in order to allow protons with energies greater than 2.5 MeV to be measured independently. The output beam current was found to be directly proportional to the input beam current, as shown in Fig. 11 [21].

Table 1  
BASIC PARAMETERS OF THE HORN DRIFT TUBE RFQ AT IFVE [21]

Injection energy.....	510 keV
Output energy.....	3.26 MeV
Frequency of the accelerating field.....	132.5 MHz
Resonator length.....	2.4 m
Outside diameter.....	0.41 m
Number of electrodes.....	65
Accelerating channel aperture.....	1.6 cm
Normalized acceptance.....	1 cm-mrad
Synchronized phase.....	30°
Resonator voltage.....	153 kV
RF pulse length.....	35 $\mu$ s
Preinjector current pulse length.....	40 $\mu$ s

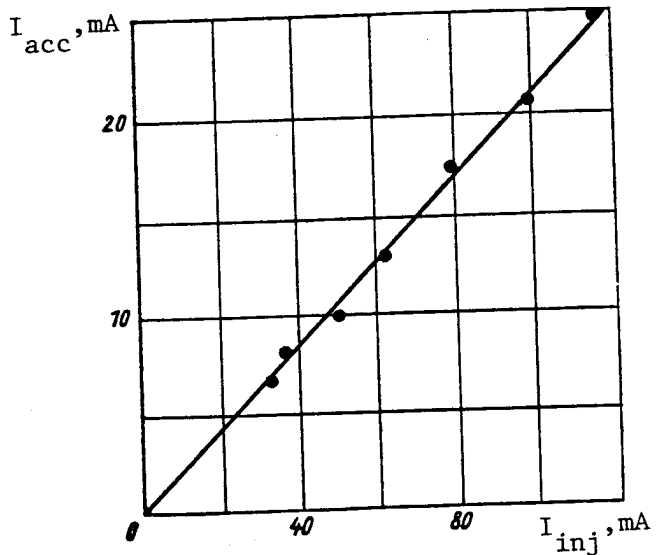


Fig. 11—Accelerated beam current as a function of injection current [21]

A maximum accelerated beam current was observed experimentally at the output of the RFQ section, as well as predicted theoretically, for a specific value of injection energy of the beam.

Using the accelerated beam current as a function of RF voltage in the resonator at a nominal value of injection energy, the IFVE researchers obtained the threshold field  $V_t$ , and thus the experimental capture coefficient ( $k_e$ ) as a function of synchronized phase, as shown in Fig. 12.

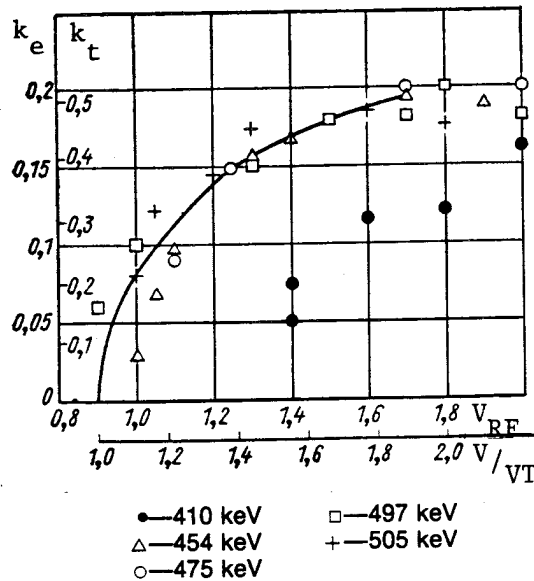


Fig. 12—Capture coefficient as a function of RF power [21]

The capture coefficient is defined here as the ratio of the accelerated particle current to the injection beam current and is represented by experimental and theoretical points in the figure ( $k_e$  and  $k_t$ , respectively). The experimental points agree well with the calculated values, as shown by the solid curve representing  $k_t$  values. From these experiments it was inferred that the capture coefficient is determined by longitudinal particle motion and is not affected by lateral particle motion.

The acceptance of the accelerator section, measured by the double slit method, had a value of  $1 \pm 0.1$  cm-mrad, as shown in Fig. 13. These measurements agreed well with the calculated values and thus showed promise that a maximum beam current of 100 mA could be reached at the accelerator output. The value  $k_e$  was 20 percent (see Fig. 12).

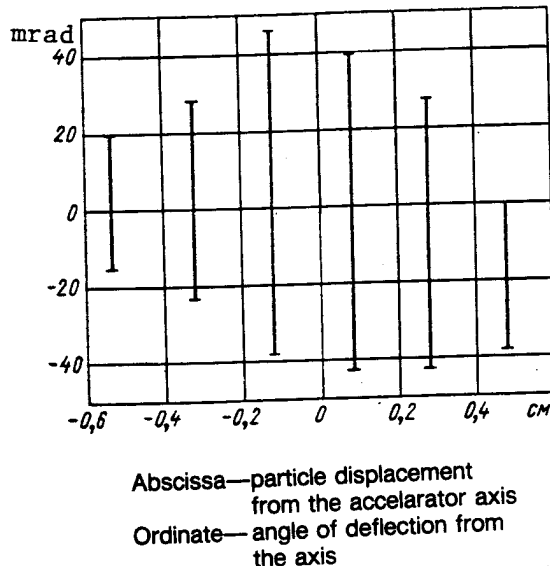


Fig. 13—Acceptance of the accelerator [21]

In these experiments the resonator consisted of a wide shield cavity in the form of a pipe with an axial slit. The drift tubes were mounted at the edge of this slit. An intermediate electrode, kept at zero potential, was inserted into the gap between the pipes. The focusing forces were created with the help of the horns at the faces of the electrodes. The acceleration electrodes were spot welded in place with the alignment of the electrodes held within 30 micrometers. The resonator elements were mounted on insulators in the vacuum chamber. A DC voltage of 2 to 3 kV was maintained between the vacuum chamber and the resonator in order to remove the electron resonance load. Owing to this construction, the RF power lead to the resonator was able to operate without voltage conditioning. The voltage in the resonator, which was almost double the rated value, could be maintained as soon as the vacuum in the chamber reached  $1 \times 10^{-6}$  Torr.

A spatially uniform RFQ system was developed and tested at IFVE in 1974 [24] and was used as the preinjector section (initial accelerator section—IAS) of the URAL linear accelerator (as described in Sec. II.4). This system utilized the four continuous electrodes as opposed to the separate horn drift tube structure described above. The maximum accelerated proton beam current at the output of the RFQ preinjector was found to be 200 mA for 400 mA injected from the ion source. The beam contained from 5 to 10 percent  $H_2^+$  ions. The beam at the RFQ

input had an energy of 100 keV and was accelerated to an energy of 620 keV.

Without the full presence of the RF field, the RFQ was able to pass the whole beam from the ion source (up to a maximum of 400 mA). In order to measure the beam current of only the accelerated particles, once the RF field was turned on, a magnetic analyzer together with a focusing lens and faraday cup was used at the output of the RFQ. The rest of the beam was lost to the analyzer vacuum chamber walls. The beam analyzing experimental apparatus is shown in Fig. 14 [24].

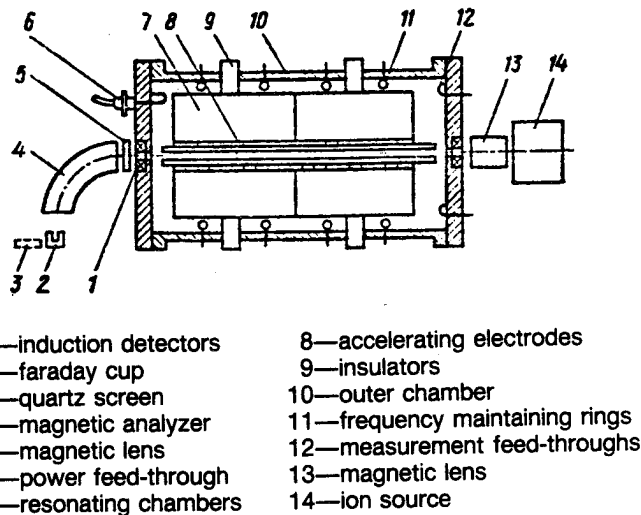


Fig. 14—Schematic of the IAS beam analyzing apparatus [24]

The dependence of the accelerated beam current upon the injected beam current and level of the RF field in the resonator is shown in Figs. 15 and 16, respectively.

The measured, as well as calculated, spectra of the accelerated proton beam are shown in Fig. 17. The stability of the beam is apparent for  $\pm 20$  percent changes in the voltage level (V) of the RF field. Adjustment of the electric field and energizing the electrodes did not cause any problems. Practically no voltage conditioning was needed in reaching the required RF voltage to establish the 158 kV/cm field.

The beam emittance was measured by photographing the imprints on a quartz screen left by beamlets sampled from the beam by a movable slit. Computer calculations were also made using this single parti-

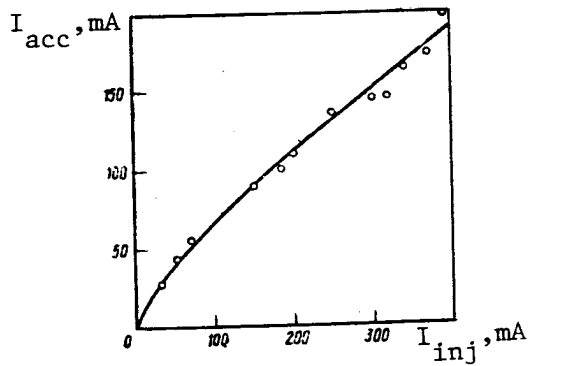


Fig. 15—Accelerated beam current as a function of injected beam current [24]

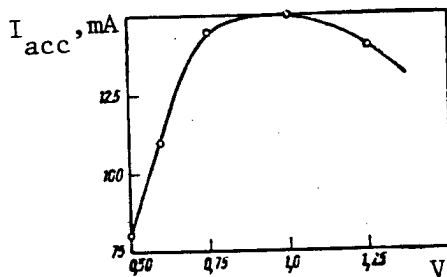


Fig. 16—Accelerated beam current as a function of the RF voltage level ( $I_{inj} = 300$  mA) [24]

cle approximation. In calculating the beam spectra, 200 axial particles were used in the beam modeling, which were evenly distributed in the input phase interval. The calculations showed that with a 6 mm beam diameter at the RFQ input and a normalized emittance of 0.35 cm-mrad, the calculated normalized emittance at the RFQ output grew, showing the definite formation of a core surrounded by a halo. The normalized emittance of the core (for 85 percent of the particles) was determined to be 0.5 cm-mrad. The emittance at the output of the RFQ was measured both for all of the particles and for accelerated particles only (see Fig. 18). The normalized emittance of only the accelerated particles by the RFQ was found to be 0.46 cm-mrad for an

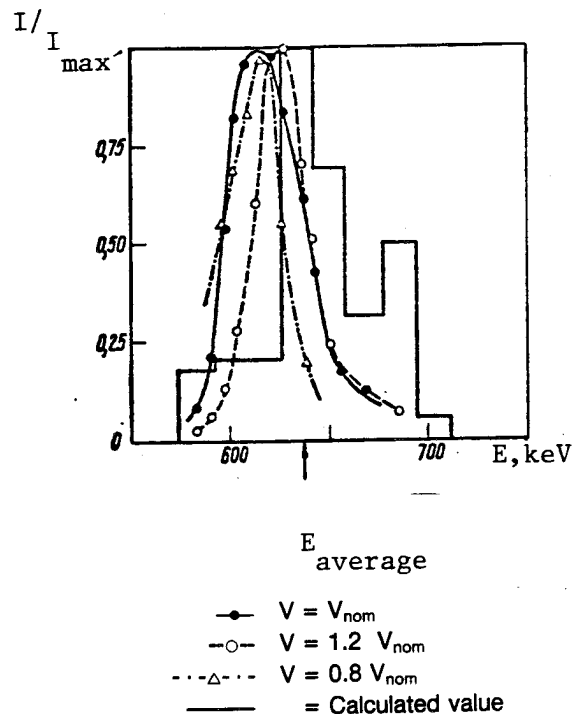
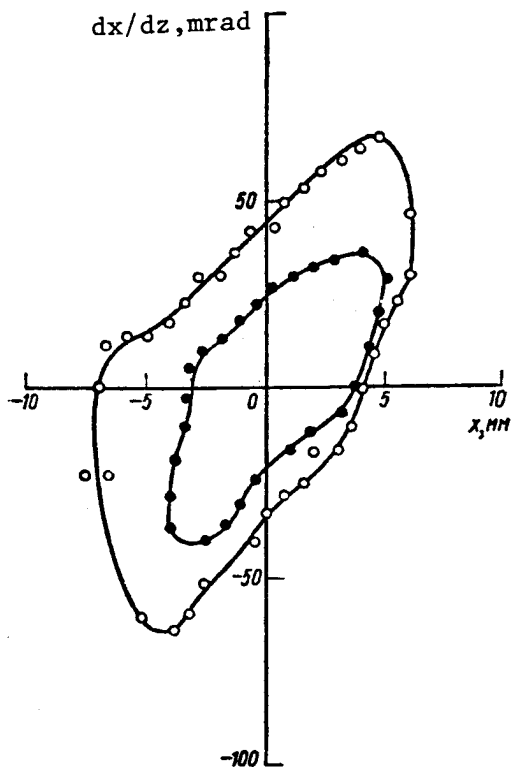


Fig. 17—Spectra of the accelerated beam [24]

accelerated beam current of 100 mA. The total normalized beam emittance for all the particles (accelerated and unaccelerated) at this beam current was 1.1 cm-mrad [24].

The basic parameters, both experimental and theoretical, of this RFQ are shown in Table 2 [24].

In 1981 IFVE studied the problem of matching the ion beam between the ion source and the focusing channel of the RFQ [25]. The acceptance of linear ion accelerators is strongly dependent upon the phase of the incoming particles as they enter the accelerating high-frequency field. This applies more to the RFQ than to magnetic quadrupole focusing accelerators [26]. In order to minimize the dependence on the phase of the incoming particles, IFVE developed a matching section located just before the RFQ. The RFQ resonator and matching section are shown schematically in Fig. 19a and the accelerating electrodes are shown in Fig. 19b. The acceptance curves for the RFQ as a function of the phase are shown in Fig. 20 [25].



- emittance of the accelerated and unaccelerated particles
- emittance of only the accelerated particles
- $I_{inj} = I_{out} = 200 \text{ mA}$
- $I_{accel} = 100 \text{ mA}$

Fig. 18—Beam emittance measurements at the output of the RFQ [24]

The mutual part of the curves (the effective acceptance) is two to three times smaller than the acceptance of any one of the separate input phases. This complicates the problems of injection. In addition, during the acceleration process, the beam emittance increases because of the mismatching of the input beam emittance, with the phase sensitive acceptance as shown in Fig. 21 [25].

To solve the problem, the matching section at the input to the RFQ should be chosen so that the system acceptance becomes less dependent upon the input phase, at least during the interval with the most predominant phases. In the matching section as developed at

Table 2  
BASIC PARAMETERS OF THE RFQ USED IN THE  
PREINJECTOR SECTION AT IFVE [24]

Parameter	Unit	Theoretical	Experimental
Injection energy	keV	100	100
Output energy	keV	635	620
Maximum accelerated particle beam current	mA	100 to 150	200
Synchronous phase	degrees	71 to 37	71 to 37
RF field frequency	MHz	148.5	148.5
Spectra pulse width	%	$\pm 0$	$\pm 7$
Normalized emittance	cm-mrad	0.5	0.46
Aperture diameter	mm	16	16
Acceleration system length	mm	1360	1360
Outer chamber diameter	mm	460	460
Voltage on resonators	kV	164	164
RF pulse width	$\mu$ s	50	50
Beam current pulse width	$\mu$ s	10	10
Pulse rep. rate	Hz	0.5	0.5
Power loss to walls	MW	0.24	0.24

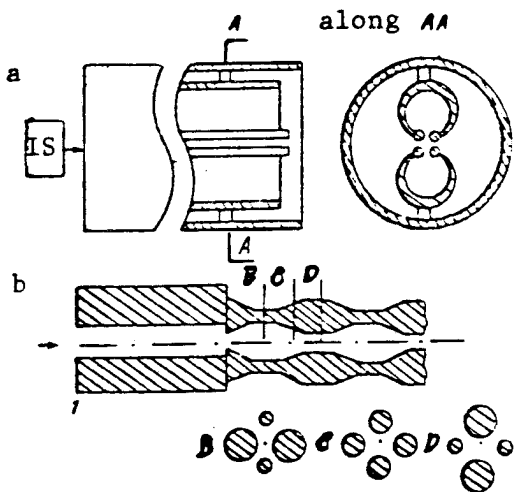


Fig. 19—RFQ electrode shape and cross-section of resonators with the matching section connected to the input of the RFQ accelerating electrodes [25]

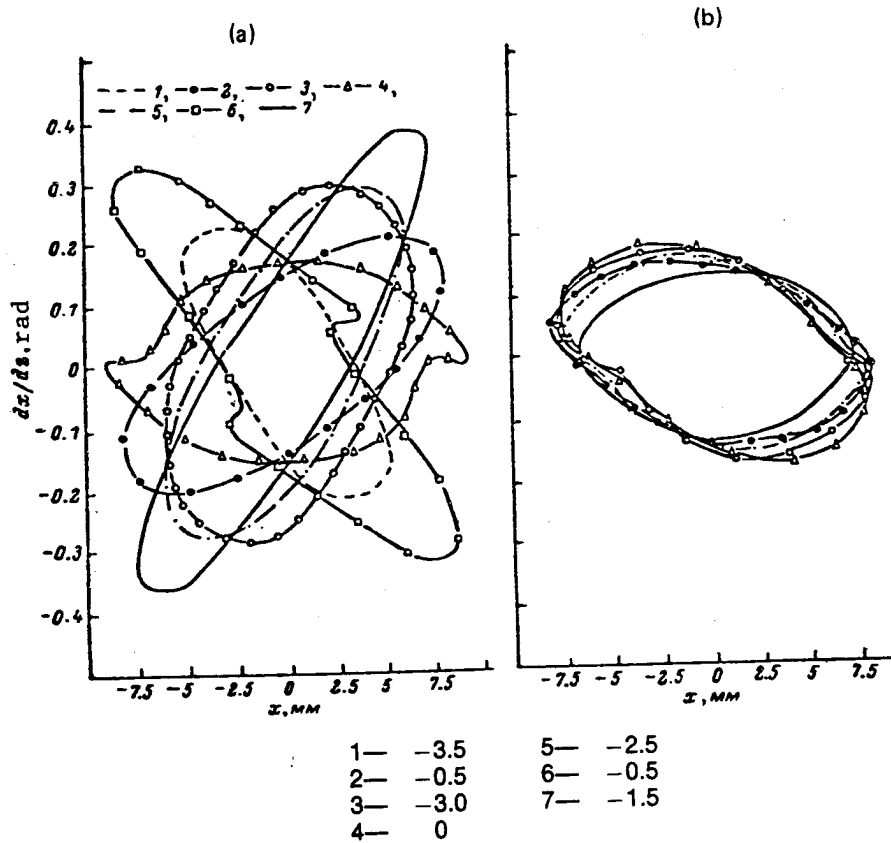


Fig. 20—RFQ acceptance curves as a function of input phase (in radians) without a matching section (a) and with a matching section (b) [25]

IFVE [27], the beam acceptance was increased by about a factor of two (compare Fig. 20b with Fig. 20a). For most of the input phases, the acceptance becomes practically independent of phase. Figs. 21b and 21a show the RFQ output beam emittance with and without the matching section, respectively. The emittance of the halo, as seen in Fig. 21b, decreased by more than a factor of two. Similar findings have been observed in other planes of symmetry. In order to increase the intensity of the accelerated particle beam, the four elements of the matching section are mounted in the accelerator resonator coaxially and flush against the four-element line. All the radial dimensions of the four-element line of the matching section are  $\sqrt{2}$  times larger than

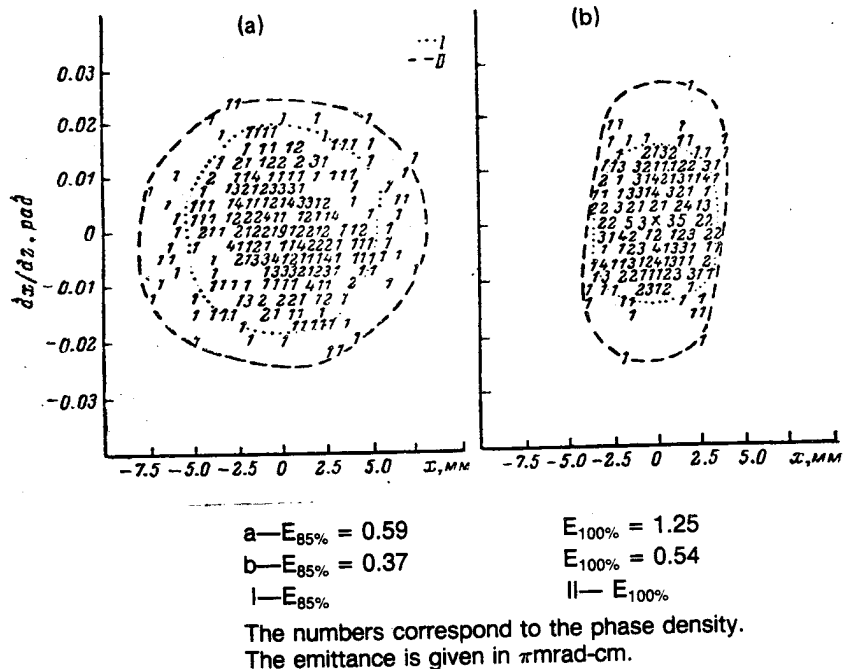


Fig. 21—Emittance diagram for a beam at the output of the RFQ for an input emittance of  $E_{\text{in}} = 0.35$  without a matching section (a) and with a matching section (b) [25]

the corresponding dimensions of the four-element accelerator line. Its length is one-half of the radial oscillation period length of the particles injected into the matching section [27].

While these results were obtained in the USSR in 1975, similar results and proposals were made independently in the West by K. R. Crandall et al. [28] in 1979 on the matching device, with a somewhat different location of electrodes but with a basically similar mode of operation.

The acceleration system of the RFQ is constructed on the base of a double H-resonator, the cross-section at which is shown in Fig. 3a. This resonator consists of two H-cavities located in one container. The cavities are loaded with cylindrical electrodes which form a four-element line and produce a homogeneous, longitudinal quadrupole RF field. Power amplifiers were used in the RF system, originally developed at RAIAN for the I-100 accelerator. Because of the small

dimensions of the resonators, the stored energy is low and the efficiency of the resonators can be higher than 70 percent [29].

The synchronous phase in the RFQ decreased adiabatically from  $\varphi_c \approx 80^\circ$  at the input to  $\varphi_c \approx 37^\circ$  at the end of the bunching section (at about 700 keV). With further acceleration to 2 MeV, the  $\varphi_c$  remains constant. The calculated value of the capture coefficient was 83 percent at a sufficiently high coulomb current limit, with the beam current greater than 200 mA [30].

#### II.4. RFQ INJECTOR OPERATION AT IFVE

Developmental work at IFVE on the injector to the proton synchrotron has been active for the last 10 years. The first stage of the linear accelerator (the URAL-15) was placed in operation in 1975. The second stage of the main accelerator was added to the URAL-15 in 1976, and the full accelerator (URAL-30) went into operation in 1977. During 1978, experimental beam runs were made, together with routine debugging of the accelerator system. In 1979, the whole accelerator was moved to the proton synchrotron injector building and remounted.

The experiments with the URAL-30 accelerator demonstrated the total system to be operational as predicted by theory and showed the satisfactory operation of the RFQ in the preinjector section. A proton beam of 80 mA, 5  $\mu$ s pulse length at 30 MeV, was obtained in 1980, with experimental beam parameters close to rated values. With the ion source beam current of 160 mA, the RFQ output beam current was measured to be 130 mA, demonstrating a capture coefficient of 65 percent. The maximum capture coefficient of the RFQ reached 83 percent. The ion source was able to produce a maximum beam current of 500 mA and operated well with a 200 mA beam with a beam emittance of 0.1 to 0.2 cm-mrad. It was determined that, at beam current values greater than 200 mA, the theoretical coulomb repulsion limit was being approached. The normalized acceptance of the main accelerator section (MAS) was greater than 1 cm-mrad, with an acceleration efficiency of 0.8 to .85. The transfer energy between the RFQ and the MAS was chosen to be 2 MeV in order to avoid the possibility of resonance between the longitudinal and lateral oscillations [31].

The overall system of the URAL-30 injector utilizing the RFQ is shown in the block diagram of Fig. 22 [30]. The ion beam is formed in the ion source, from where it is injected into the RFQ (details of which were given in Sec. II.3) and then is further accelerated by the main accelerator section (details of which are presented at the end of this section).

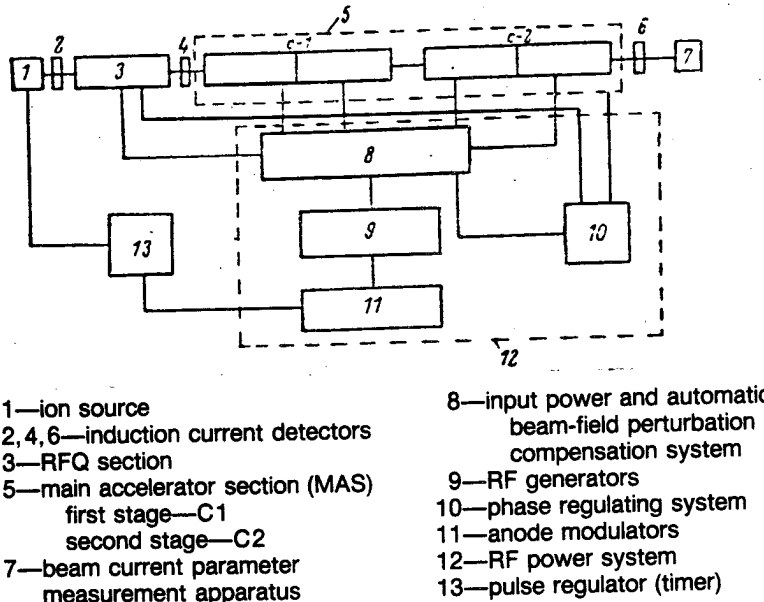


Fig. 22—Block diagram of the URAL-30 accelerator [30]

The basic values of the individual parameters of the URAL-30 system are shown in Table 3 [30].

The shape of the accelerating electrodes of the RFQ and MAS is shown in Fig. 23b, and the cross-section details of the resonators are shown in Fig. 23c [31]. The diameter of the H-resonator of the MAS is three times smaller than the diameter of the cylindrical Alvarez resonator. The transition energy between the RFQ and the MAS was chosen to be 2 MeV in order to avoid the possibility of any resonance between lateral and longitudinal particle oscillations. At 2 MeV the conditions for positioning the accelerator electrodes are considerably simplified for the first periods of acceleration in the MAS.

The acceleration and focusing of the beam in the MAS is carried out in a "double gap" which is formed by three electrodes, in which two (basic) are attached to the section of the resonating chamber of the H-resonator [32] and the third (intermediate) is kept at zero potential. The focusing quadrupole field component is created in space between the "horns," which are attached to the faces of adjacent electrodes. In the first stage of URAL-30 (up to a beam energy of 16 MeV), a non-symmetric structure with double gaps is used. The horns are not

Table 3  
BASIC PARAMETERS OF THE URAL-30 INJECTOR SYSTEM [30]

URAL-30 Parameters	RFQ	MAS	
		Stage 1	Stage 2
Injection energy, MeV	0.1	1.98	16.12
Output energy, MeV	1.98	16.12	29.87
Projected beam current, mA	100	100	100
Beam pulse spectra width, %	$\pm 3.2$	$\pm 1.2$	$\pm 0.83$
Normalized emittance, cm-mrad	$(0.5-1)\pi$	$(0.5-1)\pi$	$(0.5-1)\pi$
Current pulse width, $\mu$ s	10	10	10
Repetition pulse frequency, Hz	0.2	0.2	0.2
Generator power, MW	1.1	3.1	4.1
Operational frequency, MHz	148.5	148.5	148.5
Vessel length, m	3.5	8.7	12.7
Vessel diameter, m	0.52	0.4	0.4
Aperture diameter, mm	20.2-16.0	19.0	22.0
Normalized acceptance, cm-mrad at $\phi = \phi_c$	$1.86\pi$	$1.4\pi$	$1.4\pi$
Synchronization phase, degrees	84-37.6	30	30
Resonator voltage, kV	200	304	352

present in the first half of the gap. This structure provides acceleration and focusing components and their phasing that are more acceptable for all the particles of the pulse [22]. The second stage of the accelerator uses a symmetric double-gap structure with horns of similar length in both halves of the gap. This structure is not quite as effective as the nonsymmetric one, but is more advantageous from RF considerations of the H-resonator [30].

The H-resonator is made up of resonating chambers in the form of slit cylinders mounted on insulators in a shielding container that is about a factor of three smaller in diameter than the Alvarez-type resonator at the same operating wavelength. The URAL-30 features an auto-compensation system (described in [33]) for the compensation of excitations introduced into the RF field by the resonator.

The initial stage of the accelerator (URAL-15) was first run in May 1975 with a maximum beam current of 140 mA. At a beam current of 100 mA the normalized emittance was measured to be less than 0.25 cm-mrad (for 85 percent of the particles). The main accelerator section of the URAL-15 was first operated in December of 1975, reaching

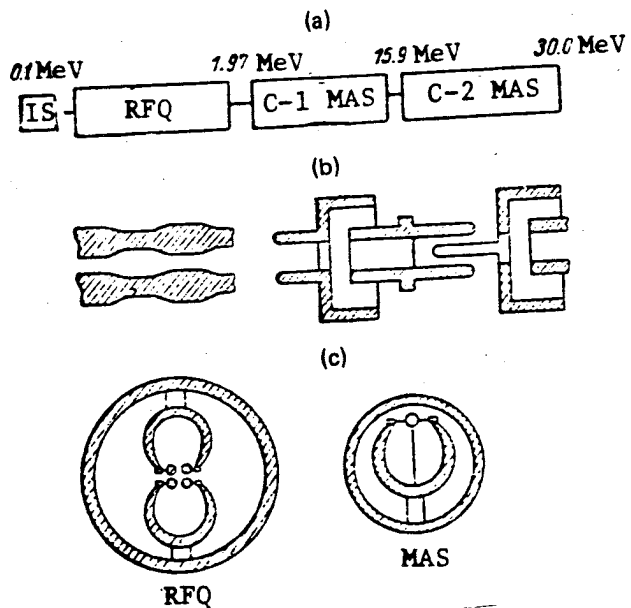


Fig. 23—Block diagram of the URAL-30 accelerator (a), electrode shape (b), and cross-section of the resonators (c) [31]

over 50 mA proton beam at 16 MeV. The normalized emittance was determined to be 0.3 cm-mrad for a 40 mA beam, as shown in Fig. 24 [31].

Beam currents in the URAL accelerator were measured using inductive detectors and a faraday cup, and the energy spectrum was determined using a pulsed magnetic analyzer with momentum resolution better than 0.2 percent. Emittance measurements were made using a movable collimating slit with multi-sectional current collectors providing measurements with an accuracy between 10 to 15 percent.

Measurements of the change in the spectra of the beam pulse after each acceleration section allow one to determine the threshold energy level and the beam energy at the output of each section. A valuable indicator for fine tuning of the system is provided by the measurement of the accelerated beam spectra at various RF field levels in the sections. This can be demonstrated by the lowering of the level in one of the sections, which reflects a broadening and translation of the spectral curve due to the excitation of longitudinal coherent oscillations, as shown in Fig. 25 [30].

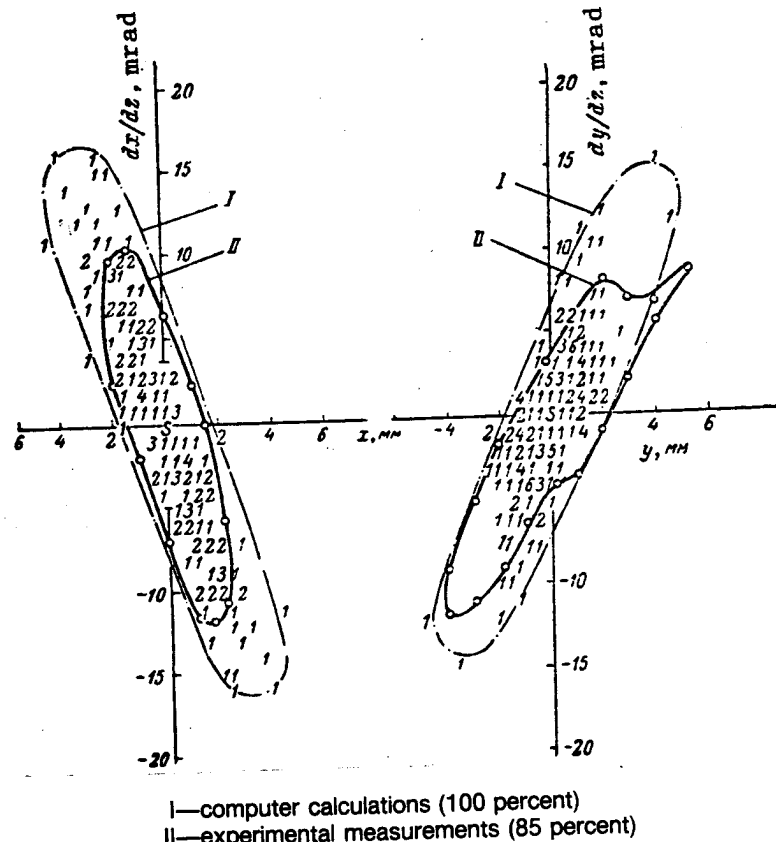


Fig. 24—Beam emittance at the output of the  
URAL-15 accelerator [31]

After determining the threshold levels of each section, the phasing of each section can be tuned more accurately. The selected injection energy was based on the accelerated beam current as a function of injection energy for different RF field levels in the RFQ. During the tuning of the accelerator system, the dependence of the accelerated beam current upon the RF voltage level in the sections was also removed.

The MAS system of the URAL-15 linear accelerator is shown in Figs. 26 and 27 using the H-resonator [34,35,23]. The H-resonator produces a mode of oscillations whose magnetic field and potential at the "slit section" do not change along the axial length.

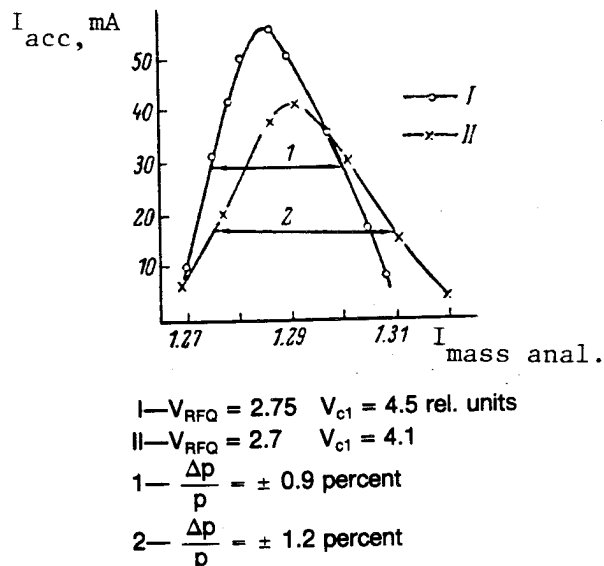


Fig. 25—Accelerated beam particle spectra at different acceleration conditions [30]

The accelerating electrodes are the double-gap type [36,22,34] and are mounted on the edge of the resonator cut. Between accelerating electrodes, an intermediate electrode is placed so that in the first gap the field is axially symmetric and in the second gap it possesses a quadrupole component. In this configuration the accelerator parameters have optimum values [22].

The measured distribution of fields in the URAL-15 accelerator along the gaps proved to be basically uniform along the accelerator system, as demonstrated in Fig. 27 [34]. The evenly spaced drops in the fields, which increase with the number of gaps passed, are due to the structure of the junctions of the resonator. Computer calculations have shown that the errors in the field distribution do not affect the operation of the accelerator. The measured average electric field in the URAL-15 was determined to be 160 kV/cm during operation, while voltage breakdown would set in at about 200 kV/cm [34].

In the investigations of the H-resonator operation and optimization of parameters, it was determined that the acceleration system possesses a higher accelerating shunting resistance than the Alvarez system (up to  $\beta = 0.15$ ); the diameter of the overall accelerating system is four to five times shorter while the rigidity is about 20 times higher. When

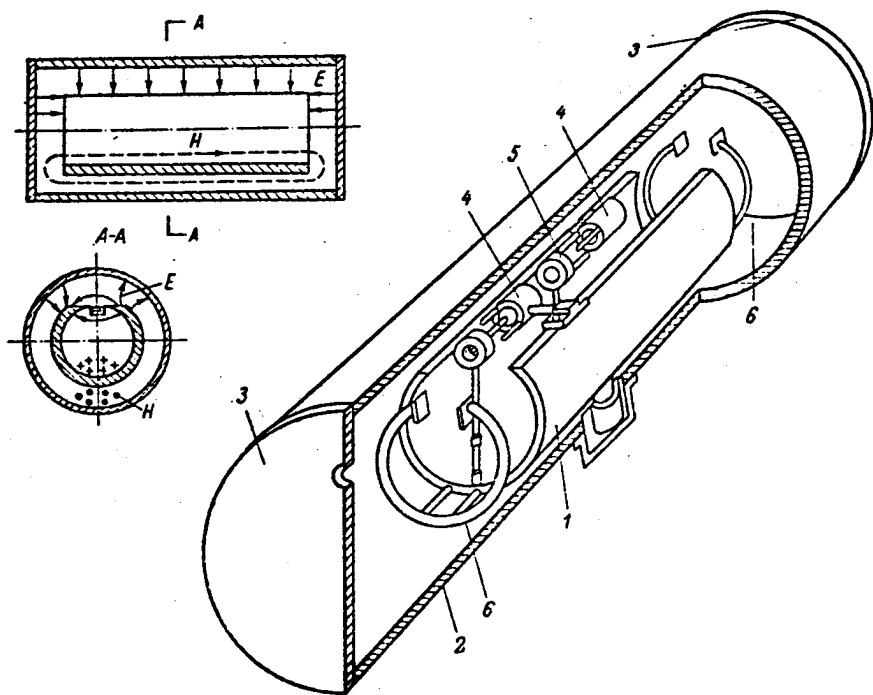


Fig. 26—The MAS accelerator system with the H-resonator [34]

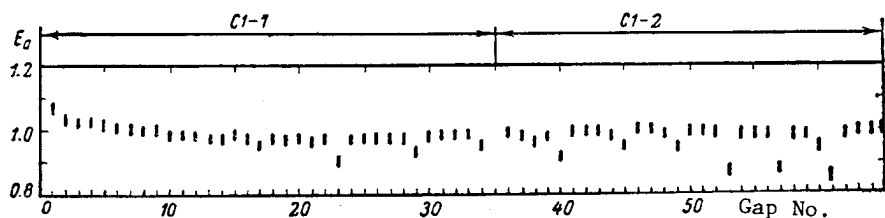
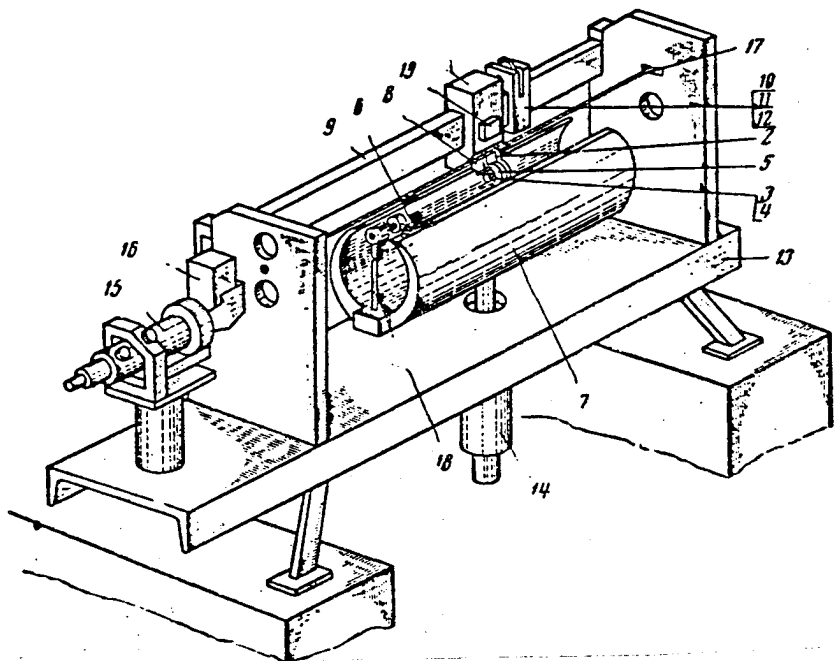


Fig. 27—Distribution of amplitudes of the applied accelerating electric field as a function of gap number along the accelerating system axis [34]

compared with the Alvarez system, this acceleration system turned out to be considerably simpler both technologically and structurally. The alignment and tuning of the accelerator system components was accomplished by a specially designed method as described in [37]. The electrodes were mounted on the axis of the resonator using a mounting stand and were attached by a special welding technique guaranteeing alignment within 30 to 40 microns. The mounting stand is shown in Fig. 28.



1—carriage	10,11,12—details of movement mechanism for carriage
2—accelerator electrode holder	13—base
3—aperture target	14—alignment mechanism
4—exchange ring	15—micro-telescope-comparator
5—mounting electrode	16—multi-prism system
6—container	17—graduated tape
7—resonator section	18—intermediate electrode rod
8—shim	19—multi-prism
9—guiding rod	

Fig. 28—Mounting stand for electrode alignment [37]

## II.5. THEORETICAL CALCULATIONS ON RFQ FOCUSING AND ACCELERATION AT IYAI

Soviet researchers state that the coulomb repulsion forces within the particle beam must be taken into account when accelerating relatively intense beam currents in a linear accelerator with RFQ focusing. However, the effect of these coulomb forces upon ion dynamics has only recently been investigated in the USSR. In 1980-1982, IYAI modeled this effect using the LINUS computer program [38,39,40]. The model was based on the "large" particle method for the initial stage of an RFQ accelerator as described in [24]. The parameters were chosen in such a way as to obtain a precise particle phase density (or emittance) at the exit of the accelerator. The calculations were made from a 16 x 16 x 32 grid with 1024 particles in half of the beam at an injection beam current of 200 mA [39]. The distribution function of the particle cloud was assumed to be Gaussian with a charge dispersion into 27 closely knit points.

As a double check on its calculations, IYAI investigated particle dynamics specifically for the case of the operating accelerator at IFVE [24]. In order to determine the effect of space charge, the characteristics of the output beam were calculated assuming both a "zero" and a 200 mA injection beam current value. The normalized beam emittance (for 85 percent beam particle sampling) was determined to be  $0.3 \pi$  cm-mrad for 200 mA beam current with a 51 percent capture coefficient. The corresponding experimental value for the emittance (with a 200 mA beam current) was  $1.1 \pi$  cm-mrad with a 50 percent capture coefficient [39]. These numbers demonstrate a strong inverse dependence of beam emittance on beam current (see Fig. 29).

Figure 30 shows the calculated beam emittance diagram at the output of the accelerator with a beam current of 200 mA. The outline represents experimental results [24].

The IYAI calculations led to a conclusion that special attention has to be given to the effects of coulomb particle repulsion in the case of intense beam currents passing through RFQ focusing accelerators.

In 1978, IYAI had created a model of the dynamics of an intense ion beam in an RFQ accelerator using part of the RF channel as a beam matching section with a continuous change in  $\mu$  from 0.2 to  $\pi/4$  in 10 focusing periods [4]. First using a "zero" beam current condition, a beam was injected into the matching section with a normalized emittance of  $0.2 \pi$  cm-mrad with a uniform particle distribution in the phase plane. The calculation showed that the matching section produced an output beam with an emittance of  $0.28 \pi$  cm-mrad, as compared with an emittance of  $0.35 \pi$  cm-mrad obtained without use of the matching section (with a 90 percent beam sampling). Further calcula-

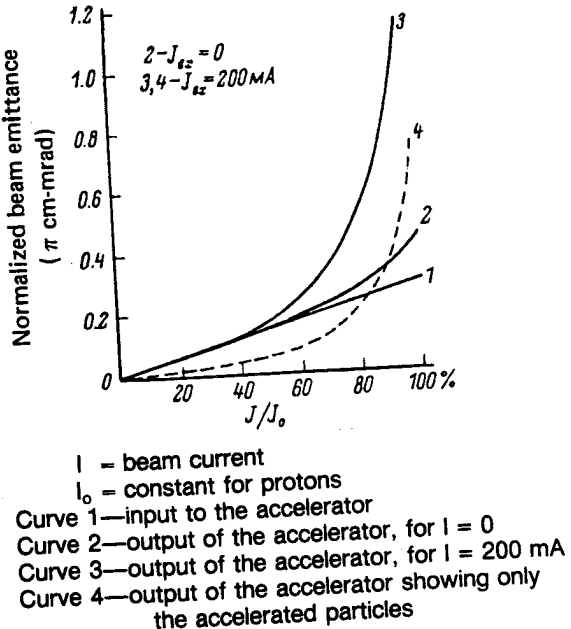


Fig. 29—Normalized beam emittance as a function of beam current [39]

tions were made with and without the matching section while assuming beam currents of 100 and 200 mA.

The beam size was also investigated as a function of distance along the accelerator axis. The results of these investigations, demonstrated in Fig. 31, show oscillations in the beam radius due to incomplete matching of the beam with the RF accelerator channel. The amplitudes of the oscillations were found to decrease toward the end of the accelerator. This decrease, especially evident at the high beam currents, was interpreted as due to the effect of nonlinearity of the coulomb and external focusing fields [40].

The quality of the beam at the accelerator output was observed to deteriorate with an increase in beam current. This is shown by plotting the partial beam emittance at the output of the accelerator as a function of injected beam current (Fig. 32).

The analysis of various beam phase profiles showed that the emittance growth basically takes place in the matching area of the accelerator. To study beam dynamics without beam matching, the beam was injected directly into the channel with  $\mu = \pi/4$ .

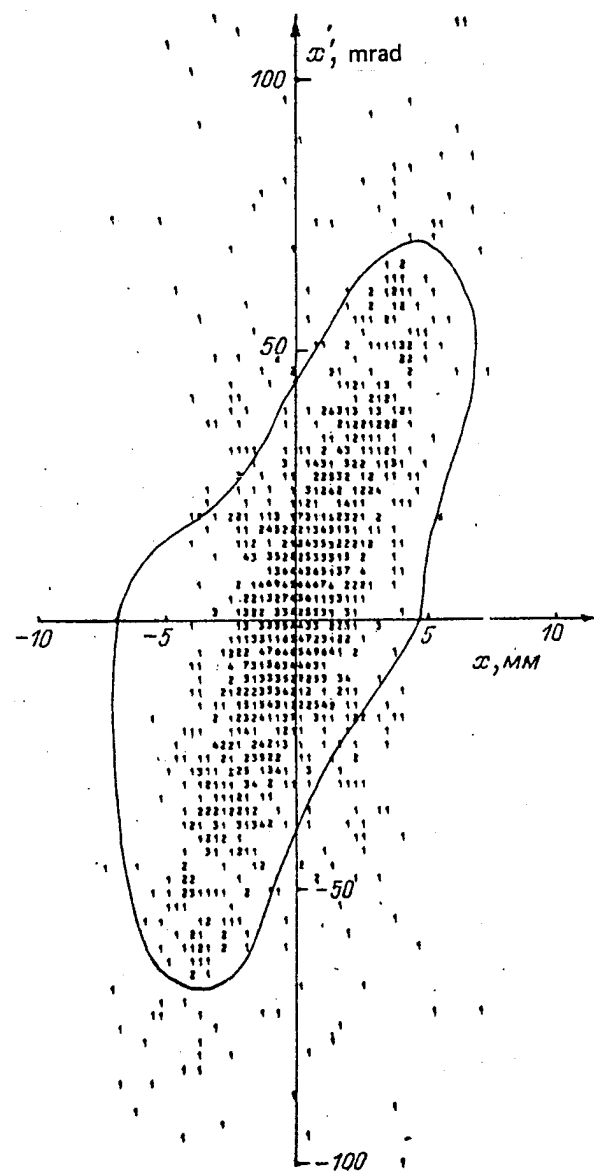


Fig. 30—Beam emittance diagram at the output of the accelerator with a beam current of 200 mA [39]

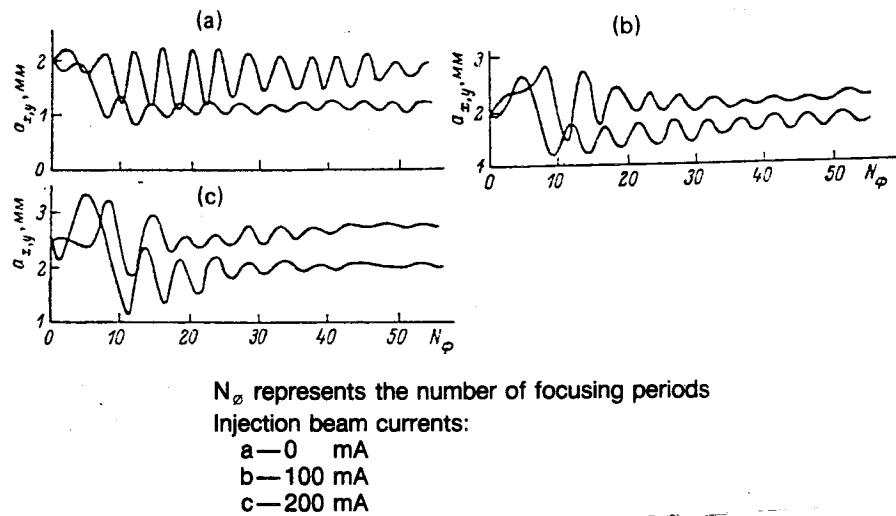


Fig. 31—Beam radius behavior along the axis of the accelerator at different beam currents [40]

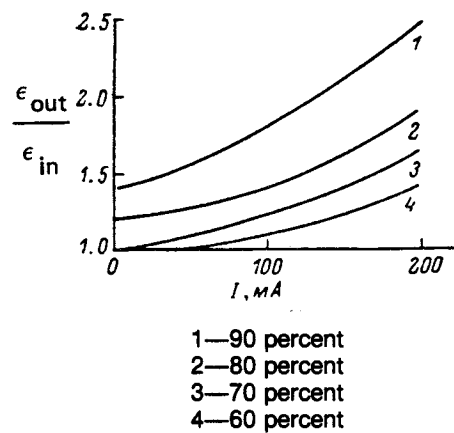


Fig. 32—Partial beam emittance at the accelerator output as a function of injected beam current [40]

A comparison of the above data showed that for a "zero" current beam, a matching section with a continuously changing  $\mu$  is effective only for low beam currents. The beam current as a function of normalized emittance is shown in Fig. 33 for an injection current of 200 mA. The solid lines represent beam matching with a continuous change of  $\mu$ , while the dashed line represents the case without matching.

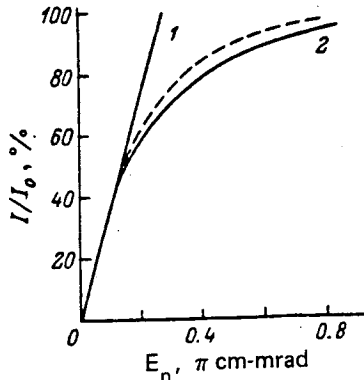


Fig. 33—Beam current as a function of normalized beam emittance at the accelerator input (1) and output (2) at an injection current of 200 mA [40]

According to IYAI, the reason for the emittance growth of the intense beam in the matching section is the insufficient focusing strength in this area. This can be verified by the results obtained from particle dynamics calculations for an RFQ accelerator using different values of  $\mu$ . With a value of  $\mu = \pi/8$  the beam emittance growth is considerably greater than with  $\mu = \pi/4$ .

In the attempt to increase the beam current of an intense ion linear accelerator, the most important issue concerns the parameters of the initial injected beam. The basic requirement in this case is the match between the injected beam and the accelerating-focusing channel of the accelerator. A mismatching can lead not only to excessive loss of ions from the beam but also to degradation in the quality of the accelerated beam.

At small injection beam currents, when the beam space charge can be neglected, the problem of matching the injection beam to the accelerator is independent both in the longitudinal and transverse

planes. The matching in the longitudinal plane is accomplished by choosing the appropriate parameters of the buncher, which would capture a maximum number of particles. The matching in the transverse plane is accomplished by fitting the four-dimensional phase space into the transverse acceptance of the linear accelerator. For this reason, computer codes [42] are used to match by minimizing the target function in many variable spaces (the parameters of the focusing fields). The problem of beam matching becomes more complex at higher beam currents, when it becomes necessary to take into account the beam's own coulomb field. Since the coulomb field combines the interaction of the motion in both planes (longitudinal and transverse), the matching of large beam currents must be considered in a six-dimensional phase space.

RAIAN has investigated the process of formation of beam bunches, taking the space charge forces into consideration by using the "large" particle method of calculation [43]. The results of these calculations showed that the presence of space charge weakens the bunching mechanism in the longitudinal plane and adds to defocusing in the transverse. RAIAN's calculations, however, have not been carried out in the six-dimensional phase space as was done recently at IYAl (see below). This is probably because the method of "large" particle calculations does not allow for such matching because it has too many degrees of freedom.

In 1980, [44] IYAl showed that six-dimensional beam matching considerably increases the effectiveness of beam injection into an intense current linear accelerator. Details of this method of calculation were reported in 1978 [45]; differential equations were then derived that allowed for the optimization of the beam-forming parameters. With the help of these equations, the external fields were checked and adjusted in the calculations using the "large particle" program. This method was used in the choice of the injector parameters of the MEGAN linear accelerator. The external fields were chosen in such a way as to provide the maximum number of particles inside the six-dimensional ellipse, the parameters of which are determined by the particle dynamics in the accelerator.

In these studies during the optimization process, it was determined that any lateral movement of the particles is very sensitive to the longitudinal bunching of the beam. The results of the calculations are shown below with comparisons of the phase-space diagrams with and without bunching while still maintaining the same focusing fields. Figure 34 shows a beam emittance diagram in one of the lateral planes with and without bunching. The ellipse in the figure represents boundaries the beam would have without bunching. It is evident that

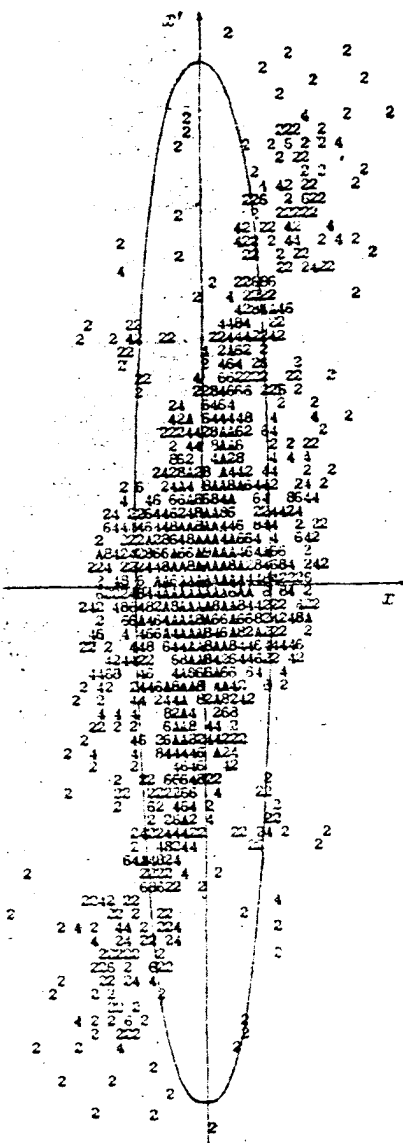


Fig. 34—Phase diagram of a bunched beam in the  $x, x'$  plane [44].

Beam current is 75 mA. The ellipse represents phase space occupied by an unbunched beam.

bunching leads to considerable beam mismatching and an increased beam emittance.

Results of the six-dimensional calculations of the particle distribution in different phase planes are shown in Fig. 35. The solid-line ellipses represent phase space obtained by maximizing the program and meeting the required demands. The individual numbers represent the corresponding phase density of the particle beam obtained by the "large particle" method of calculation. As can be concluded from the figures, there exists a maximum number of particles inside the ellipses which set the requirements. In the calculations, 4100 particles were used with a period, size, and number of "large particles" chosen in order to maintain minimum perturbation of the beam emittance.

The particle capture coefficient as a function of injected beam current is shown in Fig. 36. From the figure it can be seen that in the absence of good beam matching (curve 2) the capture coefficient decreases with increasing beam current. However, in the case of good beam matching (six-dimensional beam matching—curve 1) the data represent the optimization of the bunching fields. At optimal values of all beam focusing parameters, the capture coefficient of a well-matched beam is practically independent of beam current [44].

## II.6. DOUBLE-COMPONENT ION BEAMS

RAIAN and IYAI have also looked at the process of capture and acceleration of a "double-component" particle beam in linear accelerators [40,43], with RFQ focusing in the case of the IYAI research. The term "double component" in this case means the simultaneous acceleration and focusing of a positive and a negative ion beam, which move along the same acceleration system. In the forming and accelerating sections, these beams are spatially separated. According to IYAI, it is not sufficient to investigate the characteristics of simultaneous acceleration of the oppositely charged beams when the coulomb repulsion effects are neglected (as in the case of Alvarez-type accelerators [43]). In an RFQ accelerator with low-energy beam injection, analysis of particle dynamics must take into account the beam space charge and coulomb repulsion effects.

IYAI analyzed the longitudinal particle motion using various approximations for the coulomb particle field [40]. Initially, an  $H^-$  beam with "zero" beam current and an intense proton beam were considered. These beams were assumed to be monochromatic with an evenly distributed charge at the input to the accelerator. The beam phase profile was analyzed at various points along the accelerator axis. It was determined that in the initial stage of acceleration, where the coulomb

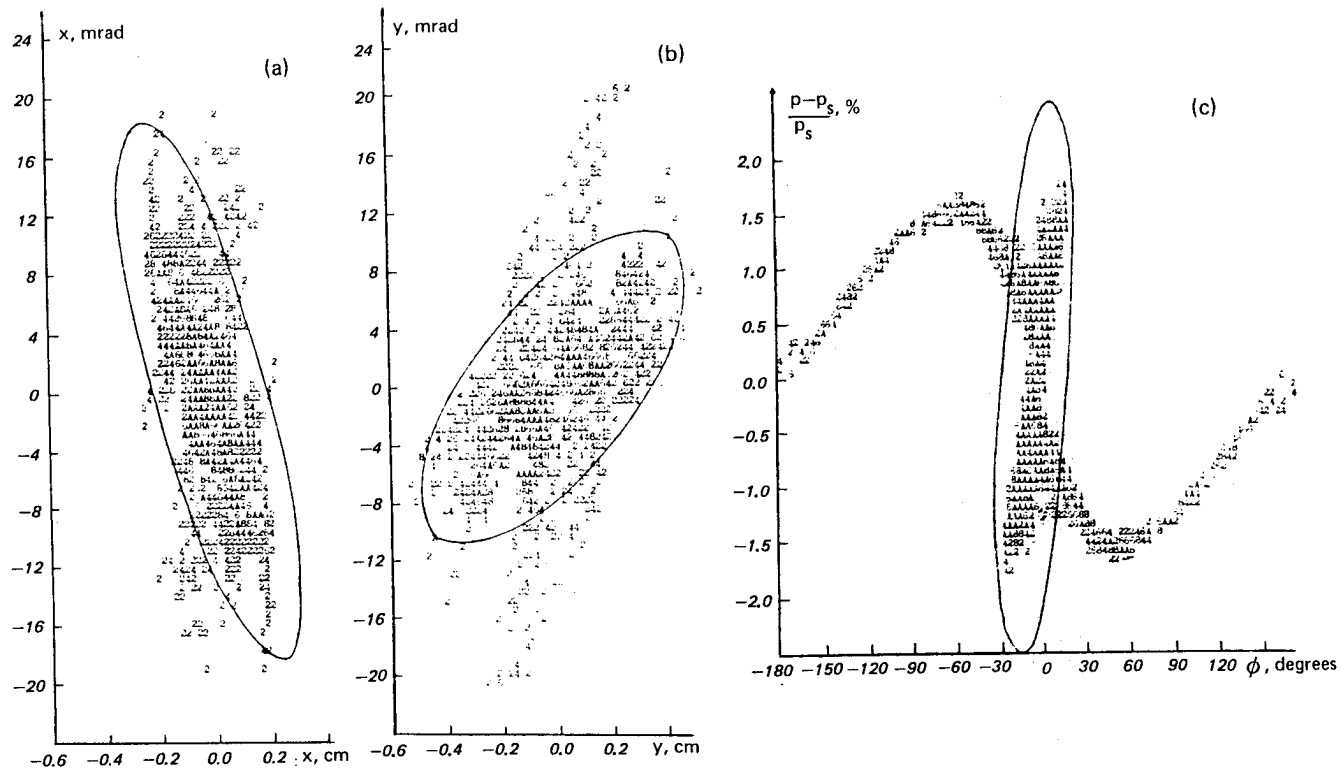
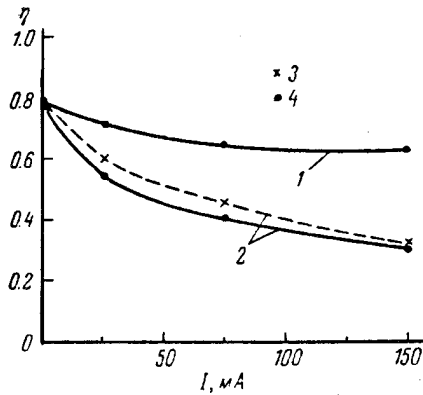


Fig. 35—Phase space diagrams showing beam matching [44]



Curve 1—6-dimensional beam matching  
 Curve 2—4-dimensional beam matching  
 Curve 3—(dashed curve x)—results of calculations obtained  
 with help of the optimization program  
 Data points—results obtained using the "large particle"  
 calculation method

Fig. 36—Dependence of the particle capture coefficient as a function of injected beam current [44]

forces are most prevalent, part of the  $H^-$  ions falls into the potential well of the proton beam. These ions are lost, however, at a later stage of acceleration. Therefore, the presence of an intense proton beam decreases the capture coefficient of  $H^-$  ions, and its coulomb field also perturbs the lateral characteristics of the weaker beam. At the end of the accelerator (at about 750 keV), however, the ion bunches are well separated and the coulomb field of the proton beam has practically no effect upon the acceleration process of  $H^-$  ions.

However, according to IYAI, the effects of the coulomb field of one beam upon the dynamics of the other will be more pronounced in the case of two intense ion beams ( $H^+$  and  $H^-$ ) of different beam currents. IYAI has also concluded that the capture coefficients of intense ion beams will be lower in the "double-component" acceleration scheme than in the case of a single beam acceleration. This can be seen by referring to Fig. 37, where the capture coefficients  $k_{H^+}$  and  $k_{H^-}$  as functions of  $H^-$  beam are affected by different intensities of the proton beam [40].

Recent theoretical investigations at IYAI were made on the non-linear interaction of intense  $H^+$  and  $H^-$  ion beams [46]. An explanation was presented on the inherent processes existing up to a period of

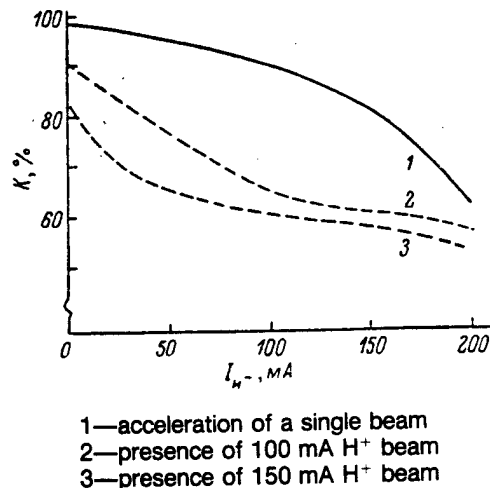
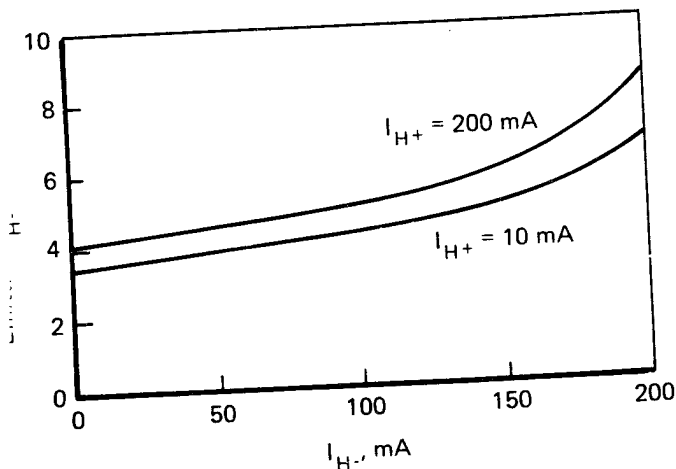


Fig. 37—Capture coefficient  $k_{H^-}$  (solid line) and  $k_{H^+}$  (dotted lines) as functions of  $H^-$  ion beam at different intensities of the proton beam [40]

about 20 plasma oscillations formed by the beams. Previously, this process has been analyzed both experimentally and theoretically for only two plasma periods [47]. These investigations have shown the possibility of obtaining ion bunches with an increase in particle density by almost a factor of 10 [46].

RAIAN researchers have made investigations on the simultaneous bunching and acceleration of  $H^+$  and  $H^-$  ion beams of intensities from 10 to 200 mA specifically for the MEGAN accelerator [48]. It was determined that the oppositely charged ion beam has an effect of perturbing the phase-space ellipse and thereby increases the emittance of the primary beam. For example, for a 200 mA  $H^-$  beam, the emittance was found to increase by 30 percent in the presence of a 200 mA  $H^+$  beam, as demonstrated in Fig. 38 [48].

In a previous Rand report [49], the author analyzed Soviet research on the formation, acceleration, and neutralization of  $H^-$  ion beams. The Soviet research presented in this report deals mainly with neutralization of negative ion beams by electron stripping in various charge-exchange targets and in background gases. No experimental data were found on  $H^-$  beam stripping at high energies, and few data are at hand



-Dependence of the effective emittance  $E_{H^-}$  at the buncher exit  
as a function of the injected  $H^-$  beam current (for  
two values of  $H^+$  beam current) [48]

acceleration in linear accelerators. No data have yet been found  
in Soviet open literature on the acceleration and focusing of  $H^-$  or  
negative ions using RFQ or APF structures.

### III. ALTERNATING PHASE FOCUSING

#### III.1. BACKGROUND AND EARLY RESEARCH ON APF

Accelerators utilizing alternating phase focusing (APF) accomplish the simultaneous acceleration and focusing of a charged particle beam pulse with only the acceleration field itself providing both radial as well as longitudinal beam stability. The acceleration of particles is accomplished by a periodic change of the polarity and magnitude of the synchronization phase along the length of the accelerator. A good introduction and review of the APF method is given in [50].

The APF focusing method was first proposed and explained by M. L. Good [51] and Ya. B. Faynberg [52]. Initially, it did not find practical application, because of the small interval in which the accelerated beam pulse experienced longitudinal and radial forces exerted by the acceleration field. The particle capture interval was determined to be small, since the accelerated particles, during the phase oscillation process, tend to fall into ineffective phases of the accelerating field, so that considerable defocusing results. It was found that the polarity-changing components of the accelerating field were unable to overcome this defocusing, and therefore the method was assumed to be ineffectual. The low particle capture coefficient thus reflects the inability to create high accelerated beam currents.

However, with the incorporation of asymmetry into the longitudinal structure of the accelerating-focusing period, the capture coefficient was increased (the phase interval widened) to a value that now is almost practical while still maintaining the axial symmetry of the fields [53,54].

The asymmetry was imposed by three different methods: first, by including a constant into the synchronous phase value [55]; later, by the periodic change of the accelerating field amplitude along the accelerator [56], or by the introduction of a special function in the synchronous phase change within the limits of the period [57,53].

The introduction of asymmetry produces an additional degree of freedom of the mutual dependence between the phasing and the focusing components of the accelerating field. Various variants of the asymmetric alternating phase focusing (AAPF) have been investigated in detail [43].

Even among the Soviet community, there seemed to be disagreement on the effectiveness of using the APF method for accelerating intense ion beams. B. P. Murin and other researchers from RAIAN had doubts as to the beam stability in the acceleration of proton beams of high intensity. These researchers showed the existence of a beam current limit of 32 mA at an energy of 1.8 MeV for the AAPF method [43]. Another analysis, taking into account space-charge forces using the "large particle" model, came up with a value of only 15 mA [43]. However, according to KhFTI, these overconservative results are due to the nonoptimal choice of the operating parameters of the accelerating-focusing channel [58]. A new method of choosing accelerator parameters for modified APF (MAPF) was first shown in 1978 at KhFTI for a deuterium accelerator, where various accelerating-focusing channel structures have been investigated in detail [59]. For the MLUD-3 accelerator with MAPF, the limiting beam current was determined to reach from 300 to 350 mA [58].

### III.2. APF RESEARCH AT RAIAN

Theoretical investigations at RAIAN in the early 1970s [56,60,61,62] demonstrated that the AAPF acceleration fields have an ability to maintain a longitudinal and lateral stability of accelerated proton bunches having particle capture phase interval greater than  $60^\circ$  to  $70^\circ$ . These calculations have been confirmed experimentally [63,62]. The experiments were carried out in 1972 [62] with an accelerator having drift tubes accelerating protons from 50 to 550 keV. The experimental measurements involved accelerated beam current, beam energy spectrum, and beam emittance. Computer calculations of AAPF interactions between phase and radial oscillations were made in 1972 [64]; the purpose was to determine the effect of these oscillations on the capture coefficients of the accelerator and the role of adiabatic damping of the oscillations and their nonlinear character in the capture mechanism. The calculations were carried out for protons in an accelerator with drift tubes using a 2 m wavelength in an energy range from 50 keV to 1 MeV.

In 1975, RAIAN [63] investigated the longitudinal and lateral motion of particles as a function of aperture diameter of an accelerator with APF in the energy range from 100 keV to 2 MeV. Soviet researchers at RAIAN believe that the acceleration of relatively large beam currents in accelerators with APF can be accomplished only with electrode apertures having large enough diameters. However, in the front-end stages of the accelerator, large apertures can cause the

accelerating field to destroy the focusing properties. By determining the accelerating-focusing channel parameters as functions of aperture size, RAIAN determined the optimum beam injection energy that should be used and thus increased the limits on the particle beam that can be accelerated. The calculations assumed a normal distribution of the accelerating field in the gaps while neglecting the effect of space charge.

In 1976, RAIAN reported a model experimental proton accelerator having the following parameters: injection energy, 100 keV; output energy, 1.8 MeV; accelerating field frequency, 150 MHz; 9 accelerating gaps; 150 kV/cm accelerating field in the gaps; particle acceleration field gradient, 5 MeV/m; length of accelerating column, 40 cm; resonator diameter, 40 cm [53]. The experimental work on this accelerator was initiated in 1976. Low-level beam currents of about 10 mA were injected and only 1 mA was accelerated at that time [53]. However, the Soviet researchers claimed that these test results showed promise for the AAPF acceleration of protons and heavy ions. In the case of extra heavy ions, such as uranium, this type of accelerator was assumed to excel any other type of accelerator.

The beam current limit for a proton accelerator with AAPF, which is imposed only by radial coulomb repulsion, has been determined at RAIAN by two methods to be 32 or 40 mA for the following parameters: injection energy, 200 keV; wavelength, 2 m; radius, 0.6 cm;  $E_m = 8 \text{ MV/m}$ ;  $\Delta\varphi_m = 20^\circ$ ;  $k_p = 1.6$ ;  $k_\varphi = 2.5$  [45].

Increasing injection energy makes it possible to increase beam aperture diameter and thus to increase beam current limit over 100 mA [61]. When the injection energy is decreased, however, the beam current limit also decreases due to radial particle repulsion.

In 1978 RAIAN analyzed a hollow beam version of the APF accelerator. According to calculations, this accelerator is capable of a maximum proton beam current of 500 mA, limited by transverse and longitudinal coulomb repulsion forces. The hollow beam mean radius was 10 cm, with an acceleration field gradient of 6 MV/m. The results showed that the acceleration of hollow beam pulses can be achieved with alternating phase focusing, with longitudinal as well as lateral particle stability in high-intensity beams [65].

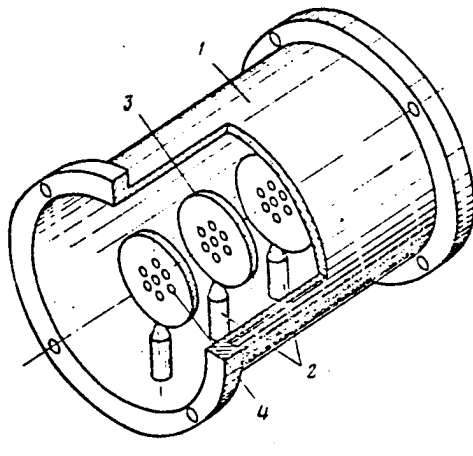
In 1977–1978, RAIAN considered an accelerator that is capable of accelerating multiple beams with AAPF. Sixteen separate beamlets were considered for a beam injection energy of 200 keV, with 16 apertures instead of the single aperture in each drift space. The distance between the axes of successive beamlets was 30 to 35 mm, and the overall diameter of the drift tube was 17 to 20 cm. The total beam current of all the beamlets was estimated to reach from 300 to 400 mA [43].

The initial accelerator section, using the 16 beamlets, provided a final energy from 800 keV to 1 MeV. Further acceleration of the beamlets beyond the 1 MeV energy point was considered by combining the 16 beamlets into four large beams, four beamlets to a beam. Each of the four large beams had a radius twice the size of the beamlets and could reach a maximum combined beam current limit of 200 mA. At this beam current level, coulomb particle repulsion did not affect the beamlet merger [43].

The four large beams were accelerated from 800 keV or 1 MeV to 20 MeV using a single acceleration tube. At 20 MeV, they were combined into a single beam with an estimated beam current from 300 to 400 mA and beam emittance of  $2.4\pi$  cm-mrad [43]. In this region of the accelerator, the current limit was higher than 400 mA and thus coulomb repulsion would also not affect the combination or further acceleration of the combined beam.

In 1978-1979, RAIAN analyzed the use of the primary section of a heavy-ion accelerator with charge-to-mass ratios of up to 1/40 in conjunction with a 500 kV injector. Singly charged argon ions were considered (with charge-to-mass ratio of 1/40 and a relativistic initial velocity of  $\beta = .005$ ) [66]. In order to obtain a relatively high intensity of the beam in the primary stages of acceleration, seven separate parallel beams were simultaneously accelerated at a field frequency of 25 MHz. It was determined that at an ion energy of 0.4 MeV/nucleon the separate beams can be combined into one composite beam which, in turn, can be further accelerated in a single channel using the same field frequency. The composite beam current of argon ions could reach 105 mA with a normalized beam output emittance of 6 cm-mrad [66]. The multiple beam design is shown in Fig. 39 using seven apertures in each drift tube to create the seven beams.

The acceleration of multiple beams can be accomplished only in the initial accelerator section, where the maximum allowable current of the accelerating channel is lower than the sum of the separate accelerated beams. When the particle velocity increases to a point where this limit no longer holds, the system of beams must be combined into a single beam to be further accelerated in a single channel. When the separate beams are combined into one, the current of the combined beam and its six-dimensional emittance increase with the number of the separate beams. The parameters of the combined beam and its emittance are dependent upon the method of beam addition [67]. A proposed method of addition is shown in Fig. 40, where the separate beams at the output of the multiple beam acceleration system (1) pass through a three-element quadrupole lens (2) which matches the lateral phase diagram



1—resonator chamber  
 2—drift-tube supports  
 3—multi-aperture drift-tubes  
 4—apertures

Fig. 39—Multiple beam accelerating structure [66]

of the combined beam with an acceptance representing a single beam accelerator (4). Beam steering plates (3), provided for each beam, steer the beams onto the mutual axis.

Figure 41 shows cross-sections of beams in the geometrical plane XY and in the orthogonal phase planes XX' and XY' before combination (a) and after (b).

The ellipse represented by the dashed lines in Fig. 41b corresponds to the effective emittance of the combined beam and has a similar shape to that of each of the separate beams. The beam is expected to be accelerated to about 1 MeV/nucleon in an acceleration channel with AAPF. The total length required for the proposed accelerator (to 1 MeV/nucleon), including the beam-combining section, should be 8.5 m.

The use of AAPF in a multi-beam accelerating system has been shown to produce relatively high-intensity beam currents with a high acceleration rate (13 MV/m) that is not attainable with other methods of focusing. It was proposed [66] that in order to achieve considerable increases in heavy-ion beam current, a multi-beam acceleration system with RFQ focusing could be used.

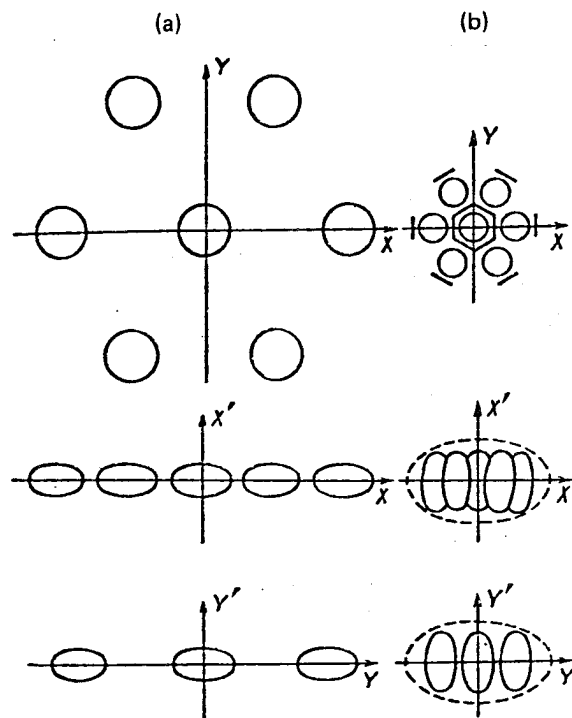
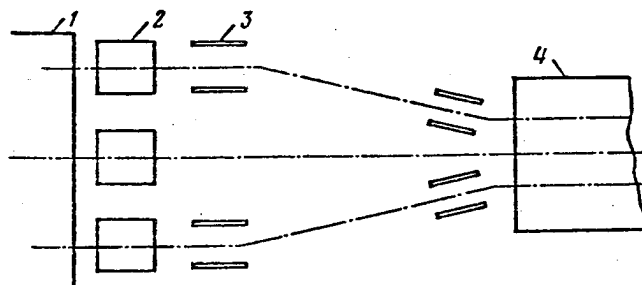


Fig. 40—Schematic of the multiple beam combination apparatus [66]



- 1—output of the multiple beam accelerating structure
- 2—focusing lenses
- 3—deflection plates
- 4—input of the combined single beam accelerating structure

Fig. 41—Diagram of the beams in the geometric and orthogonal phase planes before (a) and after (b) combination [66]

In 1978 RAIAN analyzed the magnitude of the phase and radial acceptances of a heavy-ion accelerator with AAPF which could simultaneously accelerate ions of different charges. Uranium ions introduced at the input of the accelerator at 2 MeV/nucleon would have charges from 45 to 51 and result in an output of 16 MeV/nucleon, at 4 m accelerating wavelength, and 11 MV/m accelerating field gradient. The calculations showed that particles having a charge of 46 and lower had unstable oscillations in the longitudinal direction. Particles with charges of 51 and above showed practically no stability in the lateral direction [68].

RAIAN's most recent theoretical work on AAPF was reported in 1980 [69]. The optimum mode of operation of the accelerator was determined for the case of a heavy-ion accelerator being considered for the Heavy-Ion Accelerator Complex at Dubna (UKTI). The use of seven-charge uranium ions is proposed for an output energy of 1 MeV/nucleon and an input energy of 14.7 keV/nucleon. A resonator and drift-tube accelerating structure will be used, where the RF field in adjacent gaps has opposite phases with an accelerating wavelength of 12 m and an accelerating field in the gaps of 13 MV/m. The aperture diameter in the initial part of the accelerator is 2 cm and the total length of the accelerator is 6.8 m [69]. The goal of the calculations was to maximize the longitudinal and lateral acceptances of the accelerator.

The basic feature in this optimum-designed accelerator is that the parameter of asymmetry does not remain constant but gradually changes along the length of the accelerator, as shown in Fig. 42. Here,  $\beta_s$  is the synchronous particle velocity expressed in units of velocity of light. In the optimized version of the accelerator, the constant representing the synchronous phase is about  $5^\circ$  in the direction of phasing (defocusing). Then it gradually decreases to zero, and at the end of the accelerator again reaches  $5^\circ$ , but this time in the focusing direction.

### III.3. APF RESEARCH AT KhFTI

Calculations of the accelerator particle capture in longitudinal and transverse planes were first made at KhFTI in 1977 [70], and continued in 1978 [54] and 1979 [71] under the leadership of N. A. Khi-zhnyak and N. G. Shulika. In 1980 the coulomb limit of the beam current was evaluated by numerical analysis, using the "large particle" model with space charge taken into account [58]. The analysis was

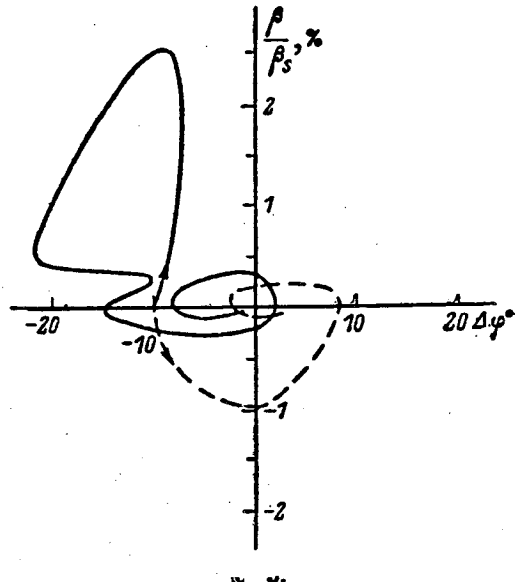


Fig. 42—Change in the synchronous phase  $\Delta\varphi$  as a function of  $\beta/\beta_s$  [69]

based on the MLUD-3 accelerator with MAPF, and showed that the limiting beam current could be as high as 350 mA [58, 72, 70].

In its most recent work on APF [72] in 1982, KhFTI studied both versions, AAPF and MAPF. A comparison of the two versions of focusing was made for the case of a 3 MeV linear deuteron accelerator. The most important parameters considered were acceleration rate, phase capture, effective channel acceptance, and maximum beam current limit.

In the analysis, the initial energy spread of the beam was taken as  $\pm 1$  percent, beam radius was 0.25 cm, the initial trajectory angle was 30 mrad, and the acceleration fields in the gaps were approximated by a square wave [58]. The lateral acceptance of the accelerator, obtained without considering space charge, is represented in Fig. 43.

The accelerated beam current was determined as a function of injected current, with a normalized beam emittance taken as 0.09 cm-mrad. This dependence is shown in Fig. 44, where the accelerated beam current initially increases almost linearly with injected current, reaches a maximum of 325 mA at 4 A injection current, and then begins to drop [58].

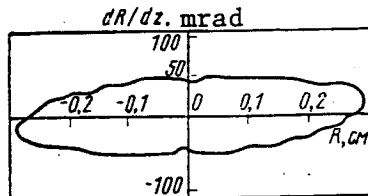


Fig. 43—Lateral acceptance of the MLUD-3 accelerator for an energy spread at the input within the limits of  $\pm 1$  percent [58]

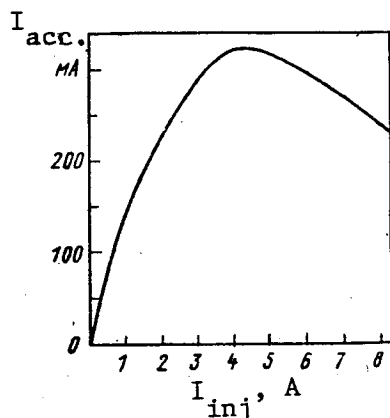


Fig. 44—Accelerated ion beam current as a function of injection current [58]

The accelerated beam current as a function of beam emittance at the input was also calculated. It is shown in Fig. 45 for an injection current of 4 A, which corresponds to the maximum accelerated beam current as shown in Fig. 44.

In the figure, the maximum particle trajectory angle (the abscissa) for a given beam radius is directly proportional to the beam emittance. Therefore, the accelerated ion beam current drops with an increase in beam emittance, because any transverse motion becomes limited owing to the beam emittance exceeding the accelerator channel acceptance.

KhFTI researchers were somewhat surprised to find the falloff of the accelerated beam current with decreasing beam emittance. Their

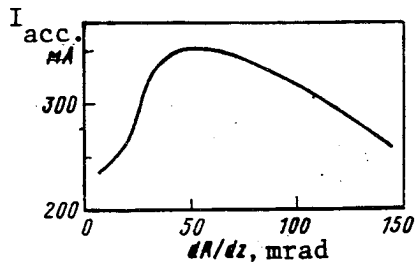


Fig. 45—Dependence of the accelerated ion beam current as a function of the maximum initial trajectory angle of the particles [58]

explanation of this phenomenon was beam overfocusing or the development of instabilities with an increase in the beam phase density [58]. The conclusion of these researchers is that the APF method could be used effectively with small linear accelerators with beam currents up to several hundreds of milliamperes and especially with accelerators utilizing heavy ions.

In the comparison of AAPF and MAPF, the MAPF system was shown to have higher rigidity [72]. Decreasing rigidity restricts the transmission of the accelerating channel and, therefore, decreases the upper limit of the accelerator beam current. In order to verify this conclusion, particle dynamics in both modes of operation were analyzed [72] using the single-particle approximation and taking into account particle-coulomb interaction.

Identical initial conditions for the injection of the particles have been imposed for both modes of acceleration, assuming an accelerating field of 90 kV/cm, an injection energy of 150 keV, accelerating field wavelength of 200 cm, and an output energy of 3 MeV. The average acceleration rate for MAPF turned out to be 1.33 times higher than that of AAPF [72]. This result can easily be explained by the fact that the lengthening of the drift-tube, which is dependent upon the transition from the positive phase to the negative phase, in the case of AAPF is made after every two accelerating periods while in the case of MAPF it is made after four or five accelerating periods. The areas of phase capture for AAPF and MAPF are shown in Fig. 46.

The extent of the phase capture area for AAPF is  $\Delta\varphi \approx 50^\circ$  while for MAPF it is  $\Delta\varphi \approx 140^\circ$ ; MAPF thus has the capture coefficient which is 2.5 times larger.

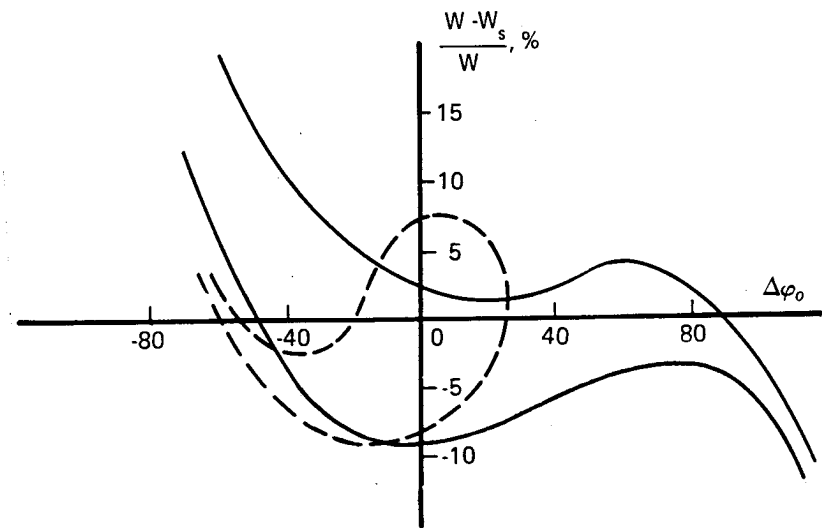


Fig. 46—Areas of phase capture for the AAPF (dotted lines) and the MAPF (solid line) cases [72]

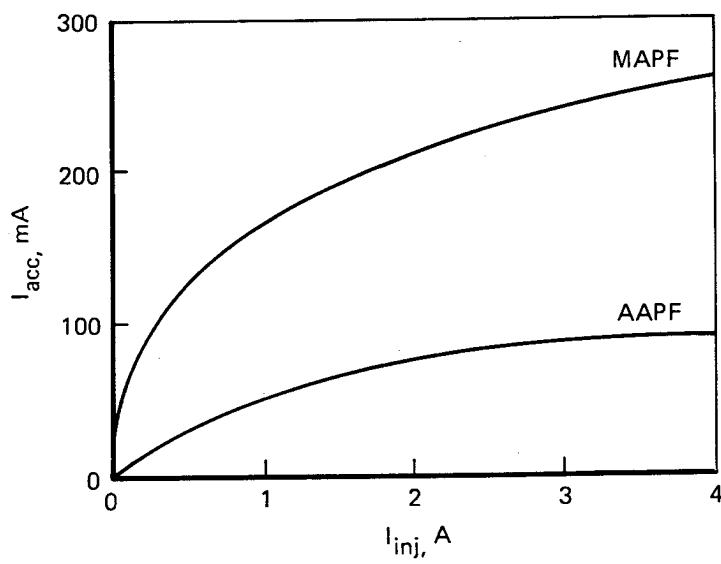


Fig. 47—Accelerated beam currents for the AAPF (bottom curve) and the MAPF (top curve) cases [72]

The effective acceptance calculated for the MAPF case was determined to be  $0.112\pi$  cm-mrad and for the AAPF case it was  $0.035\pi$  cm-mrad.

The maximum accelerated beam current was obtained for the MAPF case with a value of 250 mA, with an injected current of 4 A as shown in the top curve of Fig. 47.

It was concluded in the recent KhFTI studies that the choice of the focusing method plays a most important part in obtaining accelerated beams with optimum parameters. The use of the MAPF method results not only in an expanded phase capture region and better radial beam characteristics but also in an increased average acceleration rate. The considerable increase in the beam current limit of the accelerator makes it possible to obtain output beam currents up to 100 mA with capture coefficients of 0.25 to 0.35 [72].

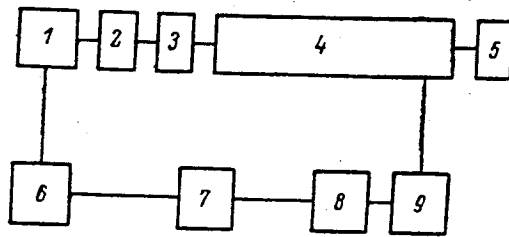
#### III.4. APF RESEARCH AT MIFI

A 1.2 MeV proton linear accelerator with AAPF was put into operation in June 1981 at the Radiation-Accelerator Laboratory of the Moscow Engineering Physics Institute (MIFI) [73]. The proton beam was formed using a duoplasmatron ion source with a directly heated cathode and operating in a pulsed gas injection mode. The beam injection energy was 100 keV with an injected beam current of up to 120 mA and beam pulse length of 150  $\mu$ s. According to Soviet researchers, the maximum beam current that can be accelerated through this accelerator has not yet been reached. Further studies are now in progress to maximize the beam current at the output.

A schematic of the overall accelerator system is shown in Fig. 48 and its basic parameters are represented in Table 4.

A single electrostatic lens was located immediately following the injector ion source which focused the beam into the accelerator and matched the beam emittance to the accelerator acceptance. The extractor electrode of the injector could be laterally translated in order to change the position of the beam for fine tuning of the accelerator. The beam cross-section at the output of the injector was measured with a double slit collimator. It was determined that about 90 percent of the beam current was found within a beam radius of 5 mm. Beam emittance, as measured with the double slit method, was determined to have a value of 0.16 cm-mrad [73].

The accelerator's distinguishing feature is the use of a double-line resonator with drift tubes having small radial dimensions, a high value of shunting resistance, and the ability to even out the acceleration field



1—ion source  
 2—fine adjustment electro-magnet  
 3—beam current detector  
 4—accelerating system  
 5—foil spectrometer  
 6—injector power supplies  
 7—timer  
 8—anode modulator  
 9—RF generator

Fig. 48—Overall schematic of the accelerator system [73]

Table 4  
 BASIC PARAMETERS OF THE 1.2 MeV ACCELERATOR  
 USING AAPF PUT INTO OPERATION AT MIFI [73]

Accelerator Parameters	Calculations	Experiment
Injection energy, keV	90	$88 \pm 2$
Output energy, MeV	1.2	1.2
Beam emittance, cm-mrad		$0.16 \pm .02$
Accelerator acceptance, cm-mrad	0.6	--
Pulse repetition rate, Hz	--	1
Top of pulse, $\mu$ s	--	$100 \pm 5$
RF pulse power, kW	84	$88 \pm 4$
Operating frequency, MHz	149.4	149.4
Resonator length, cm	74.0	74.0
Resonator diameter, cm	20.0	20.0
Aperture diameter, mm	12 to 16	12 to 16
Capture coefficient, degrees	70	--

amplitudes along the length of the accelerator. The initial development of the resonator was performed at RAIAN [74]. It demonstrated efficient operation coupled with relatively simple construction and small radial dimensions which were independent of the generator frequency. Most of the components of the resonator were made of high quality copper with the internal surfaces polished in order to optimize the RF characteristics. The schematic diagram of the resonator and beam line is shown in Fig. 49.

Half-wave oscillators (6 and 7) are mounted on supports (5) and fastened to the outer shield tank (1) with bolts (13). The connection points of opposite oscillators to the shield are displaced by a quarter wavelength relative to each other, so that the RF potential antinode is found at the end of one oscillator while it is in the middle of the other. A secondary movable support system, located next to the basic

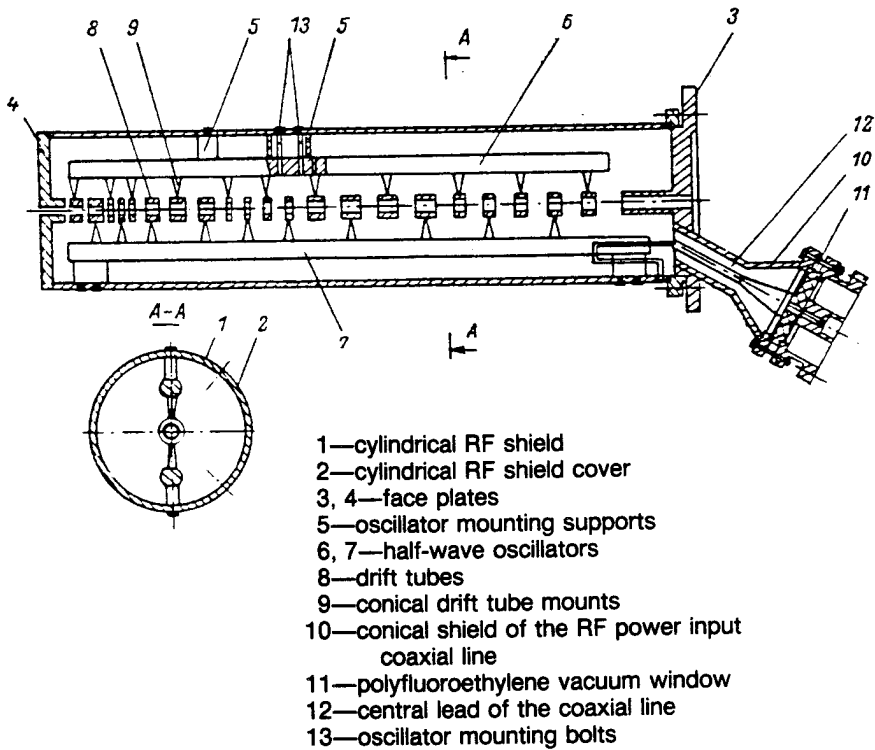


Fig. 49—Schematic diagram of the 1.2 MeV accelerator using AAPF put into operation at MIFI [73]

supports and placed near the middle of the oscillators, is used for frequency fine tuning and increases the rigidity of the oscillator. A slight movement of the supports relative to the oscillators and the outer shield shifts the resonator frequency from 2 to 3 MHz. Drift tubes (8), located along the axis of the resonator, are attached alternatively to opposite oscillators by means of conical mounts (9). The RF power input assembly is a coaxial line with conical outer shield (10) fitted with a polyfluoroethylene vacuum window (11). The central lead of the coaxial line is attached to this window.

The maximum value of the electric field fell on the center of the 17th gap and had a value of 8.5 MV/m at the rated generator RF power of 84 kW. The relative measured values of the electric fields at the centers of the accelerating gaps are shown in Fig. 50.

The beam aperture diameters, the lengths of the acceleration gaps and acceleration electrodes, and the optimum locations for electrode supports were determined by calculations based on equations of motion of charged particles in an accelerator with AAPF [43].

There were 20 drift tubes used in the resonator, their lengths varying from 5 to 40 mm. The length of the accelerating gaps increased monotonically from 6 to 32 mm. Three focusing periods along the acceleration line were 2.5, 3.5, and 4 in wavelength units. The acceleration gaps of drift tubes 1 to 5 corresponded to the first focusing period, 6 to 12 to the second, and 13 to 20 to the third. The values of the phases are shown in Table 5 for each gap number for which the equilibrium particle passes through the center of the accelerating gap [73].

The synchronous phase  $\Delta\varphi$  as a function  $\Delta\beta/\beta_s$  for the accelerator structure is shown in Fig. 51. As seen from the figure, the extent of the phase capture of the proton for the given injection energy is  $70^\circ$ .

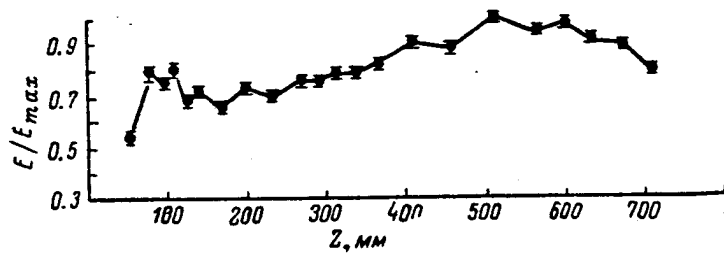


Fig. 50—Distribution of the electric field strengths along the length of the resonator [73]

Table 5  
PARTICLE PHASE VALUES FOR EACH ACCELERATION  
GAP IN THE ACCELERATOR [73]

Gap Number	Phase of Equilibrium Particle (degrees)	Gap Number	Phase of Equilibrium Particle (degrees)
1	3	11	93
2	93	12	48
3	183	13	3
4	123	14	47
5	63	15	91
6	3	16	135
7	63	17	179
8	123	18	137
9	183	19	95
10	138	20	53

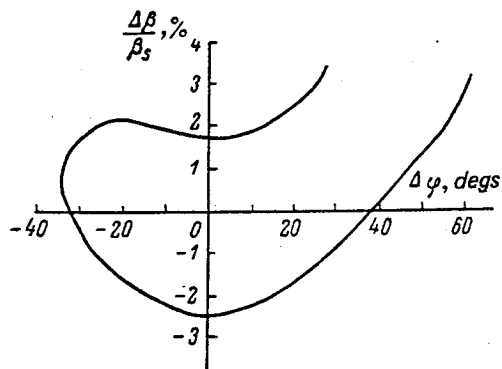


Fig. 51— $\Delta\beta/\beta_s$  as a Function of  $\Delta\varphi$  [73]

The accelerator acceptances for different injection phases of the particle  $\varphi_0$  are shown in Fig. 52. The effective acceptance is represented by the shaded area having a value of 0.6 cm-mrad.

MIFI has recently conducted additional investigation of the APF method of acceleration. This research was involved in a particular case of APF that Soviet researchers call "traveling wave field focusing" (TWFF); it explores a method of focusing particles by the accelerating field of a traveling wave as first proposed in 1957 [75], developed at MIFI in 1971 [76, 77], and further advanced recently [78, 79].

To accelerate and focus the particles, a polyharmonic system is used that employs two well-defined harmonics: one for acceleration and the other for focusing. The harmonics are created by modulating the amplitude of the accelerating field. In structures utilizing drift tubes, these drift tubes are responsible to form the required modulation of the field, as has been shown in Ref. 76. With this kind of modulation, it was determined that two more harmonics are formed in addition to the basic harmonic. These are a slow one and a fast one, whose phase velocities are correspondingly less than and greater than the phase velocity of the basic harmonic. Thus, the basic harmonic is used for

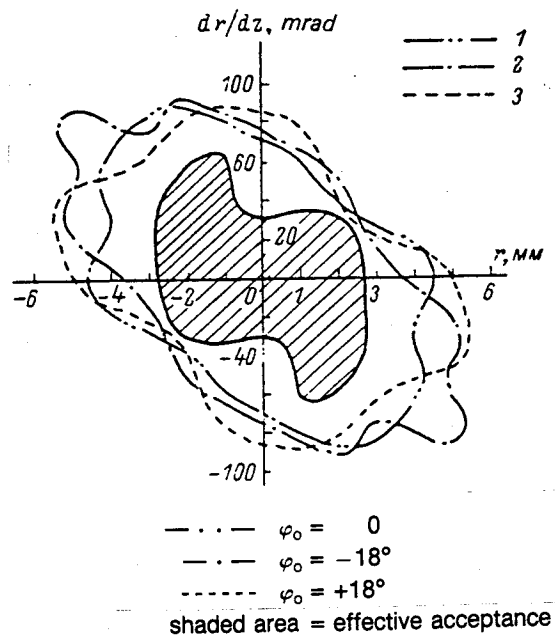


Fig. 52—Accelerator acceptances for various injection phases of the particles [73]

focusing and the slow harmonic is used for acceleration. The amplitude and the phase velocity of the acceleration harmonic are determined by the depth and the period of the modulation of the basic harmonic [78]. Several other linear accelerator variations utilizing different harmonics for acceleration and focusing have been investigated [79]; only a few of these combinations were found to be effective for the simultaneous acceleration and focusing of a particle beam.

A feasibility study was made [78] on the possible design of an accelerator using TWFF. With an initial particle velocity of  $\beta_{int} = 0.0106$ , accelerating field gradient of 14 MV/m, acceleration rate of 0.75 MeV/m, and extent of phase capture of 160°, the maximum pulsed beam current was determined to be 100 mA. The most important advantage of a TWFF accelerator was quoted to be its operation in the 2 m wavelength region, which is the most utilized region in resonant ion linear accelerators. This type of accelerator permits one to accelerate, immediately after the injector, a variety of ions (up to nickel ions having a charge of 5) [78].

#### IV. CONCLUSIONS

Soviet work on optimizing the operating parameters in the RFQ and APF structures of the ion linac systems has kept abreast of the corresponding developments in the United States. By the end of 1982, the Soviets had claimed the following basic operational performance levels for these structures:

- An RFQ proton beam current of 100 mA at 25 microsec pulse length for a 92 keV input and 3 MeV output. This development is intended for a planned 50 MeV proton linac injector.
- An RFQ proton beam current of 130 mA at 5 microsec pulse length for a 100 keV input and 2 MeV output injected into a 30 MeV linac in which the proton current reached 80 mA.
- An APF injected proton beam current of up to 120 mA at 150 microsec pulse length for a 100 keV input and a 1.2 MeV accelerator injector output.

Another significant parameter characterizing these achievements is the beam emittance, which was brought down to 0.3 cm-mrad in the 130 mA RFQ system operating alone and rose to 0.5 to 1.0 cm-mrad in this system operating with the injector stages. In the APF system, the emittance was 0.16 cm-mrad.

The Soviet parameters are comparable to the equivalent U.S. operational levels reported in U.S. publications at about the same time. For example, an average proton beam current of the order of 100 mA has been reported for the current U.S. systems, although the West, at present, is developing at least 11 accelerators using the RFQ technology.

The equivalent U.S. operational developments have been limited to the RFQ systems. The APF systems have not been used in the U.S. effort, although the Soviets claim that they are potentially significant and have shown successful operation of this system.

Parallel with the development of operating systems, the Soviet institutes have advanced several significant theoretical proposals.

Soviet research on the APF system has been characterized by a steady effort to increase the proton current up to the theoretical limit that is imposed by coulomb repulsion. At least three techniques to deal with this problem have been apparent in the Soviet open literature. First, increasing the electrode apertures was found to provide the possibility of a significant increase of the beam current above 100 mA

due to a decrease in coulomb repulsion. Second, a hollow beam APF machine has been proposed that should be capable of a proton current of 500 mA, thus significantly increasing the coulomb repulsion limit. Finally, a multiple-beam APF system was proposed as an alternative method of increasing beam current by employing multiple parallel beamlets with multiple apertures in the drift tubes. This technique is expected to provide proton currents of 300 to 400 mA for a 200 keV injection energy and final beam energy of 20 MeV.

In addition to the goal of increasing the current, the Soviet effort was directed toward expanding the region of phase capture, improving the radial beam characteristics, and increasing the average voltage gradient of the system. A modified version of the APF system is expected to triple the phase capture region, from 50° to 140°, increase the capture coefficient by a factor of 2.5, and increase the voltage gradient by one-third. These improvements are to be achieved in conjunction with a proton current as high as 350 mA.

A recent and somewhat unexpected report has it that MIFI has put into operation an APF-type accelerator with injected proton beam currents up to 120 mA and low observed beam emittance. Most of the published prior research on APF systems was either theoretical or consisted of low-current experiments, and thus did not indicate that the APF method has progressed to the point of a working prototype. Its deployment, however, seems to show that the APF system can operate successfully at higher current levels. It can be further surmised that an even more advanced APF system can be expected in the future, if KhFTI's claims for its modified APF version featuring many promising features are true.

The Soviet drive towards increasing the limit on proton current has produced a considerable body of theoretical findings in this area. Prominent in this work is Soviet stress on coulomb repulsion, which must be taken into account in the case of low input voltages and high beam currents, beam degradation and emittance that increase with beam current, and beam emittance growth that takes place at the front end of the accelerator system. The corresponding experimental work has dealt with beam emittance as a function of the phase of injected particles. Proper six-dimensional matching between the beam and the accelerator input has practically removed this dependence.

The optimum shape of the RFQ accelerating and focusing electrodes has been determined to be a half-cylinder with two different base diameters separated by a transition section with a sinusoidal profile. Problems of fabricating these electrodes have been solved, and milling machines currently perform this task in both manual and computer-controlled modes.

The overall Soviet research on both RFQ and APF methods of acceleration and focusing has concentrated exclusively on pulsed beams of protons and heavier positive ions. No evidence is available in the Soviet literature that CW operation and  $H^-$  or other negative ion beams systems are being developed in the USSR. The evidence of three operational facilities appearing in the open sources does not mean, of course, that it represents all the Soviet effort in this area and all RFQ and APF installations developed in the USSR. It is possible that other facilities exist, based on the improvements suggested in the theoretical articles published by the Soviets, and having more advanced parameters. If this is the case, the absence of these developments in the open Soviet literature could be ascribed to classification action by Soviet authorities because of possible military applications.

## REFERENCES

AE	<i>Atomnaya energiya</i>
PTE	<i>Pribory i tekhnika eksperimenta</i>
RTE	<i>Radiotekhnika i elektronika</i>
UFZh	<i>Ukrainskiy fizicheskiy zhurnal</i>
UFN	<i>Uspekhi fizicheskikh nauk</i>
ZhETF	<i>Zhurnal eksperimental'noy i teoreti-cheskoy fiziki</i>
ZhTF	<i>Zhurnal tekhnicheskoy fiziki</i>
ZhTF, Pis'ma	<i>Pis'ma v Zhurnal tekhnicheskoy fiziki</i>

1. Kapchinskiy, I. M., and V. A. Teplyakov, "Ion Linear Accelerator with Spatially Homogeneous Strong Focusing," PTE, No. 2, 1970, p. 19.
2. —, "On the Possibility of Decreasing the Injection Energy and Increasing the Beam Current Limit in an Ion Linear Accelerator," PTE, No. 4, 1970, p. 17.
3. Kapchinskiy, I. M., "Intense Ion Linear Accelerators," UFN, Vol. 132, No. 4, December 1980, p. 639.
4. Kapchinskiy, I. M., and N. V. Lazarev, "The Linear Accelerator Structures with Space-Uniform Quadrupole Focusing," *IEEE Transactions on Nuclear Science*, Vol. NS-26, No. 3, June 1979, p. 3462.
5. Vengrov, R. M., E. N. Danil'tsev, I. M. Kapchinskiy, A. M. Kozodayev, V. V. Kushin, N. V. Lazarev, A. A. Nikitin, and I. V. Chuvilo, "The Pulsed Proton Prototype of a High Current Ion Linac," *Proceedings of the 1981 Linear Accelerator Conference*, October 19-23, 1981, Bishop's Lodge, Santa Fe, N.M., LA-9234-C, February 1982.
6. Gusev, M. L., Ye. N. Danil'tsev, I. M. Kapchinskiy, S. B. Ugarov, and V. I. Edemskiy, "Investigations of a Four-Chamber H Resonator," Institute of Theoretical and Experimental Physics, Preprint ITEF-49, Moscow, 1980, pp. 1-32.
7. Kapchinskiy, I. M., V. A. Andreyev, V. S. Artemov, V. I. Bobylev, I. V. Chuvilo, E. N. Danil'tsev, V. I. Edemskiy, L. V. Kartsev, A. M. Kozodayev, A. A. Kolomyets, V. S. Kosiak, R. P. Kuybida, V. V. Kushin, N. V. Lazarev, Yu. B. Stasevich, S. B. Ugarov, and R. M. Vengrov, "The Launching of a 3 MeV Proton RFQ Linac,"

*IEEE Transactions on Nuclear Science*, Vol. NS-30, No. 4, August 1983, p. 3579.

8. Kapchinskiy, I. M., and V. I. Bobylev, "Double Frequency Proton Linear Accelerator with an Energy of up to 100 MeV," *Proceedings of the 5th All-Union Conference on Charged Particle Accelerators* (Oct. 5-7, 1976, Dubna), Vol. 1, Moscow, 1978, p. 327.
9. Kapchinskiy, I. M., "Linear Accelerator Project for a Test Neutron Generator," PTE, No. 4, 1977, p. 23.
10. Balabin, A. I., "Numerical Calculations of the Acceleration and Focusing Effectiveness in RFQ Structures," Institute of Theoretical and Experimental Physics, Preprint ITEF-54, Moscow, 1980, pp. 1-13.
11. ———, "Numerical Calculations of Fields in RFQ Structures Having Special Electrode Shapes," Institute of Theoretical and Experimental Physics, Preprint ITEF-107, Moscow, 1981, pp. 1-20.
12. Batalin, V. A., Ye. N. Danil'tsev, A. A. Zhdanko, I. M. Kapchinskiy, V. G. Kul'man, N. V. Lazarev, B. P. Murin, I. Kh. Nevyazhskiy, V. K. Plotnikov, B. I. Polyakov, and N. K. Titov, "The Proton Linear Accelerator I-2 Operating at 25 MeV," PTE, No. 5, 1967, p. 9. (Also, I-2 component information, pp. 12-71.)
13. Kapchinskiy, I. M., N. V. Lazarev, V. A. Batalin, V. I. Bobylev, A. M. Kozodayev, V. V. Kartsev, V. V. Koloskov, R. P. Kuybida, and V. I. Edemskiy, "Reconstruction of the I-2 Proton Linear Accelerator," *Proceedings of the 4th All-Union Conference on Charged Particle Accelerators* (November 1974, Moscow), Vol. I, Moscow, 1975, p. 167.
14. Batalin, V. A., I. M. Kapchinskiy, A. A. Kolomets, B. K. Kondrat'yev, R. P. Kuybida, V. S. Kuznetsov, N. P. Kuznetsova, and G. I. Trubnikov, "Increasing the Beam Current in the Proton Linear Acceleration," *Proceedings of the 3rd All-Union Conference on Charged Particle Accelerators* (October 2-4, 1972, Moscow), Vol. I, Moscow, 1973, p. 275.
15. Batalin, V. A., V. I. Bobylev, Ye. N. Danil'tsev, I. M. Kapchinskiy, A. M. Kozodayev, R. P. Kuybida, N. V. Lazarev, and V. I. Edemskiy, "Applications of the Proton Linear Accelerator I-2," AE, Vol. 33, No. 5, November 1972, p. 939.
16. Kuybida, R. P., and A. V. Kryzhanovskiy, "Proton Beam Emittance Stability at the Output of the I-2 Linear Accelerator," Institute of Theoretical and Experimental Physics, Preprint ITEF-155, Moscow, 1982, pp. 1-20.
17. Kapchinskiy, I. M., V. A. Batalin, N. V. Lazarev, V. I. Bobylev, E. N. Danil'tsev, L. V. Kartsev, A. M. Kozodayev, A. A. Kolomyets, V. V. Koloskov, V. K. Kondratyev, R. P. Kuybida, and V. I.

Edemskiy, "The Experience of Big Pulsed Current Acceleration on the Linac I-2," *Proceedings of the 1972 Proton Linear Accelerator Conference*, October 10-13, 1972, LASL, LA-5115, Los Alamos, N.M., p. 275.

18. Batalin, V. A., I. M. Kapchinskiy, A. A. Kolomets, B. K. Kondrat'yev, R. P. Kuybida, V. S. Kuznetsov, N. P. Kuznetsova, and G. I. Trubnikov, "Increasing the Beam Current in the Proton Linear Accelerator," PTE, No. 1, 1973, p. 15.
19. Kapchinskiy, I. M., "Development of the Theory and Technology of Resonance Ion Linear Accelerators," *Proceedings of the 4th All-Union Conference on Charged Particle Accelerators* (Nov. 18-20, 1974, Moscow), Vol. I, Moscow, 1975, p. 114.
20. Batalin, V. A., et al., Preprint ITEF-29, Institute of Theoretical and Experimental Physics, Moscow, 1973.
21. Il'yevskiy, S. A., I. M. Kapchinskiy, G. F. Kuznetsov, A. P. Mal'tsev, K. G. Mirzoyev, V. V. Nizhegorodtsev, V. B. Stepanov, V. A. Teplyakov, M. A. Kholodenko, and I. M. Shalashov, "Start Up of a Linear Accelerator Section with RFQ Focusing," AE, Vol. 31, No. 1, 1973, p. 56.
22. Mal'tsev, A. P., S. M. Yermakov, and V. A. Teplyakov, "Optimum Focusing Mode of an Accelerating Field," AE, Vol. 23, No. 3, 1967, p. 195.
23. Teplyakov, V. A., and V. B. Stepanov, "Investigations of an H-Resonator," RTE, No. 11, 1968, p. 1965.
24. Golosay, N. I., G. N. Dernovoy, S. A. Il'yevskiy, V. V. Klokov, N. N. Kutorga, I. G. Mal'tsev, A. P. Mal'tsev, V. S. Sevost'yanov, V. B. Stepanov, V. A. Teplyakov, and I. M. Shalashov, "Experimental Investigation on the Initial Accelerator Section Having RFQ Focusing," AE, Vol. 39, No. 2, August 1975, p. 123.
25. Dernovoy, G. N., and A. P. Mal'tsev, "RF Matching of the Beam at the Input of an Ion Linear Accelerator with RFQ Focusing," ZhTF, Vol. 52, No. 6, 1982, p. 1209.
26. Konoplev, Ye. A., and A. P. Mal'tsev, Preprint IFVE, 77-47, Institute of High Energy Physics, Serpukhov, 1977.
27. Dernovoy, G. N., and A. P. Mal'tsev, Byulletin izobretaniya, No. 30, 1978, p. 225. (Author's no. 574115.)
28. Crandall, K. R., R. H. Stokes, and T. P. Wangler, "RF Quadrupole Beam Dynamics Design Studies," Linear Accelerator Conference, September 9-14, 1979, Montauk, N.Y., p. 205.
29. Teplyakov, V. A., "Investigation of an Accelerator with RFQ Focusing," *Proceedings of the 5th All-Union Conference on Charged Particle Accelerators* (Oct. 5-7, 1976, Dubna), Vol. 1, Nauka, Moscow, 1978, p. 288.

30. Yegorov, A. A., V. A. Zenin, S. A. Il'yevskiy, S. P. Kuznetsov, A. P. Mal'tsev, I. G. Mal'tsev, V. V. Nizhegorodtsev, V. B. Stepanov, and V. A. Teplyakov, "Start Up of the Ion Linear Accelerator URAL-30," *ZhTF*, Vol. 51, No. 8, 1981, p. 1643.
31. Gorshkov, B. M., S. A. Il'yevskiy, G. M. Kolomenskiy, S. P. Kuznetsov, N. N. Kutorga, A. P. Mal'tsev, I. G. Mal'tsev, K. G. Mirzoyev, V. B. Stepanov, V. A. Teplyakov, and I. M. Shalashov, "Operation of the Proton Linear Accelerator URAL-15 with RFQ Focusing," *ZhTF*, Vol. 47, No. 11, 1977, p. 2328.
32. Stepanov, V. B., and V. A. Teplyakov, Preprint IFVE, 74-130, Institute of High Energy Physics, Serpukhov, 1974.
33. Mal'tsev, I. G., and V. A. Teplyakov, Preprint IFVE, 74-112, Institute of High Energy Physics, Serpukhov, 1974.
34. Golubkov, V. P., V. V. Klokov, V. S. Sevost'yanov, V. B. Stepanov, and V. A. Teplyakov, "RF Tuneup of the Acceleration System of the URAL-15 Linear Accelerator," *ZhTF*, Vol. 47, No. 11, 1977, p. 2332.
35. Teplyakov, V. A., and V. B. Stepanov, *Byulletin izobretaniya*, No. 14, 1968, p. 15. (Author's no. 216064.)
36. Teplyakov, V. A., "Focusing Accomplished by the Accelerating Field," *PTE*, No. 6, 1964, p. 24.
37. Stepanov, V. B., A. P. Mal'tsev, I. A. Zhuravlev, V. A. Teplyakov, and V. S. Sevost'yanov, "Alignment of the Accelerator Electrodes in an Accelerator with RFQ Focusing," *PTE*, No. 6, 1972, p. 20.
38. Ostroumov, P. N., Preprint IYAI, P-0137, Institute of Nuclear Research, Moscow, 1980.
39. Ostroumov, P. N., and A. P. Fateyev, "Effect of Space Charge upon Intense Beam Dynamics in an Accelerator with RFQ Focusing," *ZhTF*, Pis'ma, Vol. 6, No. 24, 1980, p. 1519.
40. —, "Coulomb Effects in an Ion Linear Accelerator with RFQ Focusing," *ZhTF*, Vol. 53, No. 6, 1983, p. 1082.
41. Ioffe, B. L., et al., *Proceedings of the 6th All-Union Conference on Charged Particle Accelerators* (October 11-13, 1978, Dubna), Vol. 1, Dubna, 1979, p. 236.
42. Romanov, G. V., Preprint IYAI, P-0111, Nuclear Research Institute, Moscow, 1979.
43. Murin, B. P., B. I. Bondarev, V. V. Kushin, and A. P. Fedotov, "Ion Linear Accelerators," Vol. 1, *Problems and Theory*, B. P. Murin (ed.), Moscow; Atomizdat, 1978, 264 pages.
44. Ostroumov, P. N., G. V. Romanov, and A. P. Fateyev, "High Efficiency Injection in a High Intensity Proton Linear Accelerator," *ZhTF*, Vol. 50, No. 6, 1980, p. 1237.

45. ——, "Channel Calculations for High Intensity Beam Transport," ZhTF, Pis'ma, Vol. 4, No. 13, 1978, p. 804.
46. Ostroumov, P. N., and O. V. Serdyuk, "Nonlinear Interaction of Intense H<sup>+</sup> and H<sup>-</sup> Ion Beams," ZhTF, Vol. 53, No. 2, 1983, p. 230.
47. Imshennik, V. S., et al., Preprint IPM ANSSR, Institute of Applied Mechanics, No. 41, 1974.
48. Bondarev, B. I., and V. S. Kabanov, "Effectiveness of Computation Models for the Formation of Intense Charged Particle Beams," *Proceedings of the 5th All-Union Conference on Charged Particle Accelerators* (Oct. 5–7, 1976, Dubna), Vol. 1, Moscow, 1978, p. 341.
49. Wells, N., *Production of Neutral Beams from Negative Ion Beam Systems in the USSR*, The Rand Corporation, R-2909-ARPA, December 1982.
50. Swenson, D. A., "Alternating Phase Focused Linacs," *Particle Accelerators*, Vol. 7, 1976, p. 61.
51. Good, M. L., "Phase-Reversal Focusing in Linear Accelerators," *Physical Review*, Vol. 92, No. 2, 1953, p. 538.
52. Faynberg, Ya. B., "Alternating Phase Focusing in Linear Accelerators," ZhTF, Vol. 29, No. 5, 1959, p. 568.
53. Murin, B. P., B. T. Zarubin, S. V. Zelentsov, V. S. Kabanov, V. G. Kul'man, V. V. Kushin, and N. M. Chistyakova, "Proton Linear Accelerator with Alternating Phase Focusing," *Proceedings of the 5th All-Union Conference on CPA*, Vol. 1, Moscow, 1978, p. 330.
54. Gonchar, V. Yu., S. S. Kaplin, S. A. Sapelkin, N. A. Khizhnyak, and N. G. Shulika, "Particle Dynamics Computer Modeling for a Linear Accelerator with Alternating Phase Focusing," UFZh, Vol. 24, No. 11, 1979, p. 1705.
55. Murin, B. P., et al., *Proceedings of the 8th International Conference on High Energy Accelerators*, CERN, 1971, p. 540.
56. Kushin, V. V., "Increasing the Effectiveness of Alternating Phase Focusing in Linear Accelerators," AE, Vol. 29, No. 2, August 1970, p. 123.
57. Kushin, V. V., and V. M. Mokhov, "Acceleration Field Amplitude Modulation in a Linear Accelerator with Asymmetric Alternating Phase Focusing," AE, Vol. 35, No. 3, September 1973, p. 192.
58. Beley, A. S., V. S. Kabanov, S. S. Kaplin, N. A. Khizhnyak, and N. G. Shulika, "Current Limit in an Accelerator with Alternating Phase Focusing," AE, Vol. 49, No. 5, November 1980, p. 294.
59. Papkovich, V. G., N. A. Khizhnyak, N. G. Shulika, "Alternating Phase Focusing in Linear Accelerators," *Questions on Atomic Science and Technology*, Series on Techniques on Physical Experiments, Khar'kov, No. 2(2), 1978, p. 51.

60. Dreval', I. D., and V. V. Kushin, "Conditions for the Existence of Two Stable Equilibrium Phases in Linear Accelerators," AE, Vol. 28, No. 5, May 1970, p. 423.
61. Kushin, V. V., and I. D. Dreval', "Particle Beam Current Limit in Linear Accelerators with Alternating Phase Focusing," ZhTF, Vol. 41, No. 3, 1971, p. 598.
62. Kushin, V. V., B. T. Zarubin, V. V. Svirin, and I. M. Chistyakova, "Proton Linear Accelerator Having an Energy of 550 keV with Asymmetric Alternating Phase Focusing," PTE, No. 6, 1972, p. 15.
63. Kabanov, V. S., I. D. Dreval', V. V. Kushin, and L. L. Filipchikov, "Calculated Parameters of an Accelerator with Alternating Phase Focusing with a Low Injection Energy," ZhTF, Vol. 46, No. 7, 1976, p. 1484.
64. Dreval', I. D., and V. V. Kushin, "Particle Motion Numerical Calculation in an Accelerator with Asymmetric Alternating Phase Focusing," ZhTF, Vol. 42, No. 9, 1972, p. 1915.
65. Kushin, V. V., and P. A. Fedotov, "Beam Current Limit Estimates for a Hollow Beam in Linear Accelerators with Alternating Phase Focusing," ZhTF, Pis'ma, Vol. 4, No. 5, 1978, p. 258.
66. Kushin, V. V., B. P. Murin, and P. A. Fedotov, "Multi-Beam Heavy Ion Accelerator with Alternating Phase Focusing," PTE, No. 2, 1981, p. 25.
67. Guseva, K. I., V. V. Kushin, and B. P. Murin, Trudy Radiotekhnicheskovo Instituta AN SSSR, Moscow, No. 30, 1977, p. 21.
68. Koshkarev, D. G., V. V. Kushin, and P. A. Fedotov, "Multicharged Ion Beams in Linear Accelerators with Alternating Phase Focusing," ZhTF, Pis'ma, Vol. 5, No. 6, 1979, p. 341.
69. Garashchenko, F. G., V. V. Kushin, S. V. Plotnikov, L. S. Sokolov, I. V. Strashnov, P. A. Fedotov, I. I. Kharchenko, and A. V. Tsulaya, "Optimum Conditions for Acceleration of Heavy Ions in Linear Accelerators with Asymmetric Alternating Phase Focusing," ZhTF, Vol. 52, No. 3, 1982, p. 460.
70. Baranov, L. N., et al., "Experimental Investigations of a Small Deuteron Linear Accelerator with Alternating Phase Focusing," *Questions on Atomic Science and Technology*, Series on Linear Accelerators, Khar'kov, No. 2(5), 1977, p. 12.
71. Beley, A. S., S. S. Kaplin, N. A. Khizhnyak, and N. G. Shulika, "Longitudinal Motion in a 3 MeV Proton Accelerator with Alternating Phase Focusing," ZhTF, Vol. 51, No. 3, 1981, p. 656.
72. Beley, A. S., S. S. Kaplin, N. A. Khizhnyak, S. A. Shestopal, and N. G. Shulika, "Specific Characteristics of Alternating Phase Focusing," UFZh, Vol. 27, No. 8, 1982, p. 1132.

73. Abramenko, N. I., A. N. Antropov, V. K. Bayev, V. A. Vlasov, A. P. Volkov, N. M. Gavrilov, R. K. Gavrilova, Ye. V. Gromov, V. N. Dronin, V. P. Zubovskiy, I. S. Kosyrev, S. A. Minayev, A. V. Nesterovich, I. B. Nikitin, A. N. Puchkov, V. V. Rassadin, V. V. Semenov, S. S. Stepanov, N. R. Tushev, and A. V. Shal'nov, "Proton Linear Accelerator with Alternating Phase Focusing with an Energy of 1 MeV," ZhTF, Vol. 53, No. 5, 1983, p. 858.
74. Gryaznov, N. A., A. I. Likharev, V. M. Pirozhenko, and I. B. Seleznev, *Proceedings of the 7th All-Union Conference on Charged Particle Accelerators* (1980, Dubna), Moscow, 1981, p. 51.
75. Tkalin, V. S., ZhETF, Vol. 32, 1957, p. 625.
76. Gavrilov, N. M., and V. P. Zubovskiy, "Investigation of Radial Stability in a Drift Tube System with Peripheral Magnetic Coupling," ZhTF, Vol. 41, No. 5, 1971, p. 1012.
77. Gavrilov, N. M., and A. V. Shal'nov, Moscow Engineering Physics Institute Scientific Conference (October 11-20, 1971), Moscow, 1971, p. 8.
78. Bayev, V. K., and S. A. Minayev, "Effectiveness of Ion Focusing in a Linear Accelerator with the Help of a Traveling Wave Field," ZhTF, Vol. 51, No. 11, 1981, p. 2310.
79. Bayev, V. K., N. M. Gavrilov, S. A. Minayev, and A. V. Shal'nov, "Resonant Ion Linear Accelerators with Axially-Symmetric Accelerating Field Focusing," ZhTF, Vol. 53, No. 7, 1983, p. 1287.





RAND/R-3141-ARPA

